JOURNAL OF NEUROTRAUMA 36:2558–2578 (September 1, 2019)

DOI: 10.1089/neu.2017.5574

Frequency-Dependent Changes in Resting State Electroencephalogram Functional Networks after Traumatic Brain Injury in Piglets

Lorre S. Atlan and Susan S. Margulies

Abstract

Traumatic brain injury (TBI) is a major health concern in children, as it can cause chronic cognitive and behavioral deficits. The lack of objective involuntary metrics for the diagnosis of TBI makes prognosis more challenging, especially in the pediatric context, in which children are often unable to articulate their symptoms. Resting state electroencephalograms (EEG), which are inexpensive and non-invasive, and do not require subjects to perform cognitive tasks, have not yet been used to create functional brain networks in relation to TBI in children or non-human animals; here we report the first such study. We recorded resting state EEG in awake piglets before and after TBI, from which we generated EEG functional networks from the alpha (8–12 Hz), beta (16.5–25 Hz), broad (1–35 Hz), delta (1–3.5 Hz), gamma (30–35 Hz), sigma (13–16 Hz), and theta (4–7.5 Hz) frequency bands. We hypothesize that mild TBI will induce persistent frequency-dependent changes in the 4-week-old piglet at acute and chronic time points. Hyperconnectivity was found in several frequency band networks after TBI. This study serves as proof of concept that the study of EEG functional networks in awake piglets may be useful for the development of diagnostic metrics for TBI in children.

Keywords: EEG; functional network; pediatric brain injury; porcine; resting state

Introduction

Traumatic brain injury (TBI) is the leading cause of death and disability in children in the United States.[1,2] Children have the highest incidence rates of emergency department visits associated with TBI, often as a result of sports or recreation activities.[2] Following pediatric TBI, typical symptoms include cognitive and behavioral deficits that are dependent on injury severity, location (diffuse or focal), and recovery duration. There is a great need for improved multimodal clinical assessment of pediatric TBI, because there are at present no standardized biomarkers for its diagnosis and prognosis either in the clinic or on the sidelines of a sports field.[3]

Electroencephalography (EEG) is a useful tool for examining the functional integrity of neuronal networks in health and disease. It is relatively inexpensive and non-invasive, and can provide a functional assay with high temporal resolution. In contrast to functional neuroimaging methods, a reasonable signal-to-noise ratio can be obtained even with minor subject movement, making it a particularly attractive means of evaluation in pediatric populations. However, conventional EEG is limited in its diagnostic and prognostic capability for pediatric TBI. Although there are EEG changes following severe TBI,[4] the standard clinical interpretation of EEG signals is insensitive to mild TBI (mTBI): most EEGs are within normal limits or show very subtle alterations.[5,6] Also, abnormalities in EEG signal amplitude and latencies do not consistently correlate with long-term symptoms.[6] As a way of overcoming these limitations, network analyses of EEG recordings may provide a robust and objective platform for interpretation. Functional networks are commonly utilized in the study of neuropsychiatric disorders such as stroke and schizophrenia,[7–9] and may similarly be helpful in determining the source of cognitive and behavioral deficits seen in TBI patients, including non-communicative children.

EEG recordings acquired while the subject is in a ''resting state'' are commonly analyzed using functional networks in order to study neurological disorders in humans.[10–14] ''Resting state'' typically involves subjects sitting with eyes closed in a dark room while awake and free from any overt stimuli. Resting state EEG data are easier to collect and simpler for the subject than task-based procedures, which is appealing to the study of pediatric populations, from whom cognitive tasks can be more difficult to elicit consistently and reproducibly. At the time of this publication, there were a few studies on developmental changes in resting state EEG functional networks,[10,11] but there are no reports on the effect of TBI on the pediatric human population.

Recently, the use of pigs in neuroscience research has grown because the pig brain is very similar to that of the human in anatomy and growth. Piglets share a similar rate of myelination and cerebral

Department of Bioengineering, University of Pennsylvania, Philadelphia, Pennsylvania.

hemodynamics and metabolism with human neonates.[15,16] Additionally, piglet brain development resembles the human postnatal developmental sequence as measured by EEG.[16,17] EEG patterns in the piglet in the awake state and after cerebral insult were similar to those observed in children.[17–19] The use of the 4-week-old piglet model permits investigation into the effects of TBI on EEG functional networks during early childhood (1–3 years old). We hypothesize that mTBI will induce acute and chronic, frequency-specific changes in the resting state functional connectivity of juvenile piglet brains.

In this study, we examined resting state EEG functional networks across several frequency bands in awake piglets before and after mTBI. Our data show significant frequency-dependent changes in the characteristics of networks 1, 4, and 7 days after TBI, which may be helpful for the assessment of whether TBI has occurred in the pediatric population. The novel work presented here addresses an important gap in the current EEG functional network literature on the study of pediatric TBI. Our goal is to develop a biomarker that indicates when mTBI has occurred.

Methods

Diffuse TBI in piglets

All experimental protocols were approved by the Institutional Animal Care and Use Committee of the University of Pennsylvania. Piglets were housed separately in cages and kept on a 12 h light–dark cycle. We studied seven 4-week-old, female Yorkshire piglets (neurodevelopmentally equivalent to a human toddler).[20] The pathophysiology of TBI in piglets compares well with that of human children[21,22] because of the similarities in gyral pattern, overall brain shape, and distribution of gray and white matter.[23–25] Three piglets were randomly assigned to the injured group and four were assigned to the sham group. Each piglet in the injured group sustained a single, rapid, closed-head, non-impact rotation in the sagittal plane with mean peak angular velocity of 131 rad/sec. The well-characterized diffuse white matter injury was induced via a HYGE™ pneumatic actuator,[26–28] and the angular velocity was recorded using an angular rate sensor (ATA Engineering Inc., Model#: ars-06, Herndon, VA) and a data acquisition system implemented in LabView (National Instruments, Austin, TX). Sham piglets received all of the procedures except the injury, including the anesthetic regimen. Anesthesia and analgesia were administered only on the day of injury. Buprenorphine (0.02 mg/kg) was delivered intramuscularly for analgesia prior to injury. Then, the following protocol was performed: pre-medication with intramuscular injection of ketamine (20 mg/kg) and xylazine (2 mg/kg), induction with 4% inhaled isoflurane in 1.0 fraction of inspired oxygen via snout mask until lack of reflexive pinch response, and maintenance at 1% inhaled isoflurane via endotracheal tube with fraction of inspired oxygen to 0.21 on the day of injury (day 0). Body temperature, blood pressure, oxygen saturation, heart rate, respiratory rate, and end-tidal CO_2 were continuously monitored. A circulating water blanket was kept to maintain core body temperature between 36 and 38°C. For each animal, EEG data was acquired 1 day prior to injury and 1, 4, and 7 days post-injury.

EEG data acquisition

Before beginning EEG data acquisition, piglets were acclimated to wearing a nylon sleeve in their cages for a minimum of two 30 min sessions over 2 days. Acquisition of resting-state EEG only occurred in non-agitated, silent, awake piglets using the 32 channel net (Electrical Geodesics, Inc. HydroCel™ Geodesic Sensor Net, Electrical Geodesics, Inc. Net Amps 400 EEG amplifier). The net was placed in potassium chloride electrolyte solution (11 g dry potassium chloride, 1 L water and 5 mL baby shampoo) before it was placed on the head. The International 10–20 EEG system[29] was utilized to ensure consistent positioning of the scalp electrodes (in the net) for each animal across days. We also used the nasion and inion as anatomical landmarks to ensure consistent sensor net placement across all animals. In order to maintain contact between electrode and scalp, we placed two thin nylon sleeves over the net. Before acquisition, the impedances of all electrodes were verified to be below 50 kΩ; placement of the electrodes took $\sim$7 min per piglet. We then recorded 1.5 min of continuous resting state EEG data from immobile piglets in a silent room without any movement of nearby objects or investigators. EEG data were acquired at a rate of 1 kHz and referenced to channel 33 (located at the midline in the center of the head). Recordings were discarded and repeated if background noise or head movement was observed in the same pig.

Alpha band filtering was performed on the EEG signal using the Net Station Tools 4.6 software by applying a finite impulse response bandpass filter at 8–12 Hz (passband gain: −0.01 dB, stopband gain: −40 dB, roll-off: 0.99 Hz). Frequency band limits for the beta (16.5–25 Hz), broad (1–35 Hz), delta (1–3.5 Hz), gamma (30–35 Hz), sigma (13–16 Hz), and theta (4–7.5 Hz) bands were chosen based on the study by Modarres and colleagues.[30] EEG recordings are influenced by electrical and physiological artifacts, electrode placement, skull defects, anesthesia drugs, and subject alertness.[31–33] Cellular devices were not permitted in the study room during EEG recording and the 60 Hz (electrical noise) frequency was eliminated using a notch filter. After frequency filtering, artifact detection in and removal from EEG signals was performed using a user-defined algorithm in MATLAB®.

Our artifact detection algorithm removed variations in EEG voltage caused by bad channels (eye blinks and minor movements) and replaced these short segments with the mean EEG voltage without artifacts. We excluded the first and last second of each recording to remove any artifacts arising at the start and end of the data acquisition process. We then calculated the moving average (with span 80 ms) of the EEG signal. Within sequential 500 ms segments, the minimum (min) and maximum (max) moving average EEG values were computed. A segment of EEG signal was deemed to contain an artifact if its max-min value exceeded the threshold value of 20 μV, which was determined by manual inspection to robustly flag artifacts across all channels and animals. Artifacts accounted for 20.5% of the EEG recordings. We calculated the number of artifacts for injured and sham piglets across days and found that shams (20.4% ± 0.79%) had mean/standard error percent of EEG signal with artifact similar to those of the injured piglets (20.6% ± 0.93%). There was no difference in the level of artifacts in the EEG for injured and sham piglets.

Average spectral power and mean frequency analysis

We then calculated average spectral power and mean frequency to illustrate changes in EEG features that were the result of injury. Spectral power was calculated using the Fulop & Fitz method,[34] in MATLAB,[35] after applying a Hanning window to the 1.5 min preprocessed EEG signal from all 32 electrodes. The average power of the post-processed (frequency-filtered and artifact removed) EEG signals was taken over the 1–35 Hz range of interest. We also calculated the mean frequency power-weighted average over the 1–35Hz range for every frequency band. Mean frequency was calculated as: $\sum_i f_i * power_{norm,i}$, where f_i denotes the ith frequency value in the 1–35Hz domain and $Power_{norm,i}$ is the normalized power (power at f_i divided by the sum of power values across all frequencies). One scalar value of average power and the mean frequency were determined for each electrode at every frequency band; every animal contributed 32 average power and mean frequency measures. We used short-term fast Fourier transform analysis over the 1.5 min epoch and pre-defined narrowband ranges

to identify mean frequency and power changes via methods that are consistent with previously published studies.[36–40]

Construction of EEG functional networks

Networks are collections of nodes and edges. The 32 electrodes can be regarded as representing the nodes, and the synchrony between them can be regarded as representing the edges. The resulting functional networks can provide insight into the interactions among the various brain regions over which electrodes are placed. Functional networks were constructed by calculating network edges as the maximum absolute cross-correlation of the amplitudes of the EEG signals between all pairs of electrodes (Fig. 1). One edge between two nodes represents the similarity between EEG signals from both nodes. Every 1.5-min-long EEG recording was segmented into short (1000 ms) segments, and one network was built for each segment, yielding ~88 undirected, weighted EEG functional networks per animal per study day (Fig. 1). This analysis approach used is similar to that used by Chu and colleagues.[36] All of the networks calculated were fully connected; that is, had 496 edges among 32 nodes and were not thresholded for analysis in order to include the information from all edges. The broadband networks for all post-injury days were compared to the pre-injury day for sham and injury groups by constructing 32×32 matrices. Networks were calculated for the alpha (8–12 Hz), beta (16.5–25 Hz), broad (1–35 Hz), delta (1–3.5 Hz), gamma (30–35 Hz), sigma (13–16 Hz), and theta (4–7.5 Hz) bands.

EEG functional network metrics

Network metrics were then calculated in order to quantify the integration (global communication and cooperation among brain regions) and segregation (formation of local and functionally specialized modules among brain regions) properties as well as the influence of key nodes and edges on the network. The four metrics calculated were: nodal strength, clustering coefficient, global efficiency, and modularity. Nodal strength was calculated as the sum of edges that each electrode has to all other electrodes. Clustering coefficient was calculated as the geometric mean of edges that formed triangles around each node. Nodal strength and clustering coefficient are node-based metrics, meaning that there is a single value of nodal strength and clustering coefficient for each electrode; median values of nodal strength and clustering coefficient from all 32 electrodes were taken to yield a single, representative measure of nodal strength and clustering coefficient for each EEG network. The median values provide a network-wide measure of connectivity; that is, not specific to node location. Global efficiency was calculated as the average inverse of the shortest path length between all possible pairs of nodes in the network, where a path is the sequence of distinct edges taken to traverse nodes throughout

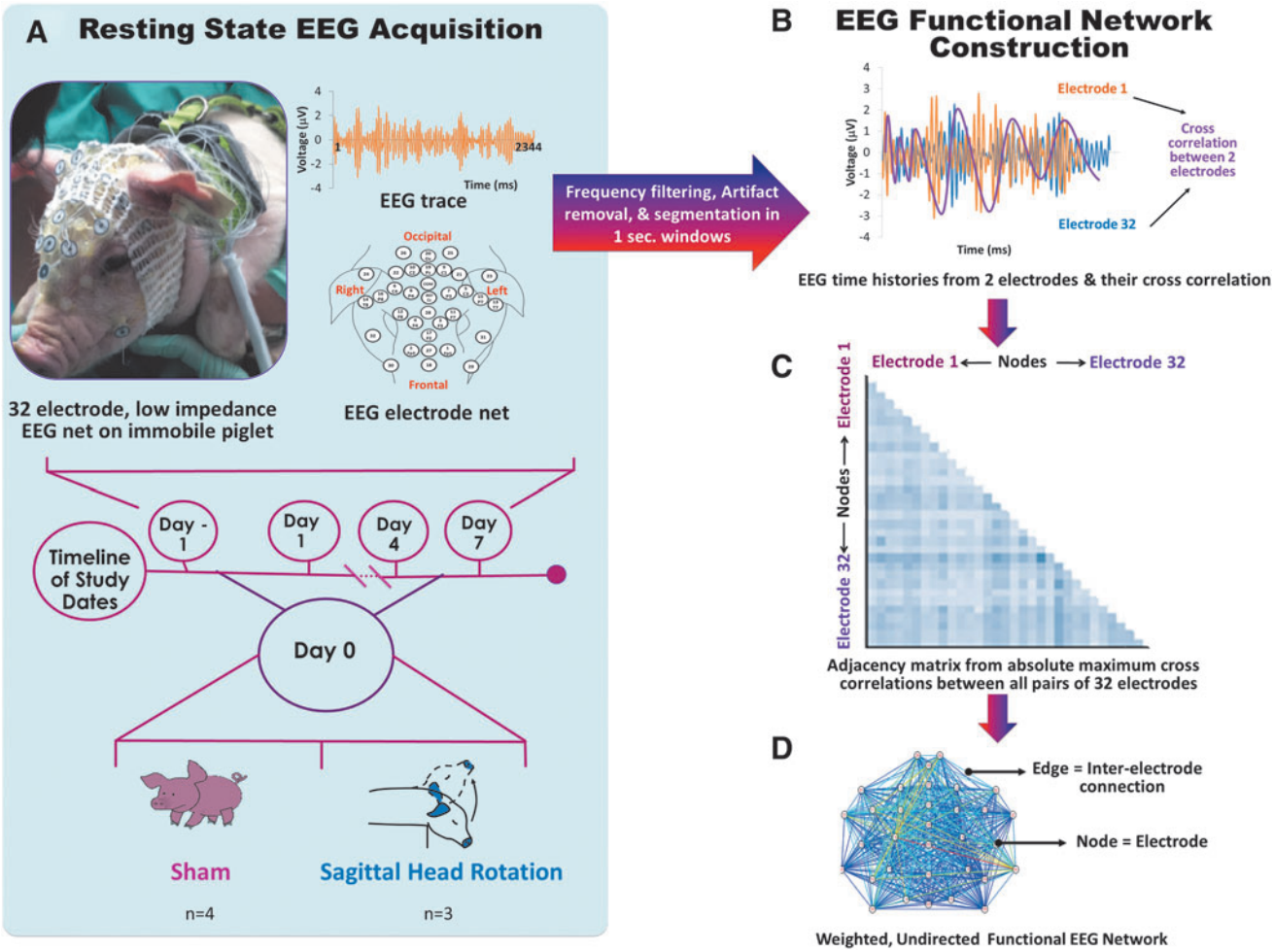

FIG. 1. Diagram showing **(A)** resting-state electroencephalogram (EEG) acquisition from sham and injured piglets and **(B)** network construction from all pairwise cross-correlations, which form **(C)** an adjacency matrix that indicates the strength of inter-electrode connections across the brain that may also be represented as **(D)** a weighted EEG functional network.

the network. Modularity is the degree to which a network's nodes and edges may be separated or combined. Modularity was calculated using the MATLAB Brain Connectivity Toolbox[37] with the Louvain–greedy algorithm, with the modularity resolution parameter set as 1 (the classic value).

Analysis of core EEG functional network topology

Changes in the weighted EEG functional network metrics may be the result of changes in the strength of edges, the number of connections, or both. In order to determine the source of changes in networks, we examined whether network topology or the arrangement of the core edges changes after injury. The method used was based on that performed by Chu and colleagues.[36] Each weighted, cross-correlation network (captured from 1000 ms of EEG data) was converted to a binary network by statistical thresholding of its edges. One sided empirical p values were determined for each edge in the weighted network by counting the number of edges that were greater than the edge considered and dividing the count by the total number of edges in the network.[41] Edges with significant p values ($p < 0.05$) formed a binary network representation of the strongest neural connections throughout the network over the 1000 ms epoch. In a single animal, all binary networks were summed across time to obtain a weighted, consensus network over the 88 sec duration of resting state EEG recording. We extracted the most persistent edges present over the total EEG recording duration by finding edges in the consensus network with weights above the 95th percentile. The strongest 5% of edges were calculated for all animals and frequency bands.

Statistical analysis

We utilized a non-parametric Dunnett's test[42] to compare all metrics from post-injury (POST 1, 4, and 7) days with those from the pre-injury (PRE) day, with a significance level of 0.05. The logarithm was taken of all network metrics (except modularity) before statistical tests were performed. Statistical tests were applied to all spectral power and network metrics for all frequency bands. All statistical analyses were performed in R 3.4.1[43] using the nparcomp package.[44] For all boxplots, the box plot height is defined by the 25th and 75th percentiles (1st and 3rd quartiles). The upper whisker is the largest observation ≤ the 75th percentile $+1.5\times$ IQR (where IQR is the interquartile range, or distance between the first and third quartiles). The lower whisker extends to smallest observation ≥ the 25th percentile - $1.5\times$IQR. Data beyond the end of the whiskers are called ''outlying'' points and are plotted individually.

Results

Effect of TBI on spectral power

We classified the EEG signals into human EEG frequency bands, specifically the alpha (8–12 Hz), beta (16.5–25 Hz), broad (1–35 Hz), delta (1–3.5 Hz), gamma (30–35 Hz), sigma (13–16 Hz), and theta (4–7.5 Hz) bands. Across frequencies, there were large and significant alterations in the average spectral power in the injured group compared with the sham group (Fig. 2, summarized in Table 1). Generally, there was little change in the spectral power in the sham group. We focused our attention on those bands and time points with no change in sham, and significant changes after TBI. In the alpha frequency band (8–12 Hz), we observed no significant changes ($p > 0.05$) in average spectral power in the sham group on any POST day compared with PRE (Fig. 2A). In the injured group, there was a significant increase ($p < 0.0001$) in alpha power on POST 1 day and reductions on POST 4 and 7 days ($p < 0.0001$) compared with pre-injury levels. There was no change ($p > 0.05$) in average beta (Fig. 2B) power in the sham group on any day relative to PRE anesthesia; however, beta power increased significantly ($p < 0.0001$) POST 1 d compared with its PRE value, and returned to its PRE value by POST 4 day. Reductions ($p < 0.01$) in broadband and delta (Fig. 2C and D) average power values were observed in the sham group on POST 1 day relative to PRE. In the injured group, there were reductions in broadband ($p < 0.01$) and delta power ($p < 0.05$) POST 1, 4, and 7 days relative to PRE. Although no significant changes ($p > 0.4$) in power were seen in the theta band (Fig. 2E), for sham, reduction ($p < 0.03$) in power was seen in the injured group on POST 1, 4, and 7 days compared with PRE. In the sham group, a decrease ($p < 0.01$) in gamma power (Fig. 2F) was noted on POST 1 day ($p = 0.0004$), whereas an increase was observed in the injured group on POST 1 day ($p < 0.047$), in addition to decreases on POST 4 and 7 days. Average power in the sigma band (Fig. 2G) decreased ($p < 0.01$) on POST 7 days in the sham group compared with PRE, whereas injury caused an increase ($p < 0.0001$) in sigma power on POST 1 day. In summary, whereas there were both increases and decreases in spectral power 1 day after TBI, we observed consistent and persistent decreases in broadband, delta, theta, and gamma spectral power measures on 4 and 7 days post-injury that were not observed in the sham group.

Effect of TBI on mean frequency

Small, but significant injury and time-dependent changes in the mean frequency across all frequency bands were observed (Fig. 3, summarized in Table 2). Elevation of the mean alpha frequency ($p < 0.006$) was seen on all days after sham treatment, whereas no change ($p > 0.05$) was seen on POST 1 day and decreases ($p = 0.0036$) were noted in the injured group on POST 4 and 7 days (Fig. 3A). The mean frequency in the beta band (Fig. 3B) was elevated ($p < 0.0001$) on POST 1, 4, and 7 days compared with PRE in the sham group in contrast to the reductions ($p < 0.0001$) on all POST days in the injury group. There were increases ($p < 0.05$) in the broadband mean frequency (Fig. 3C) in sham and injured groups on POST 4 and 7 days relative to PRE; the injured group had significant increases ($p < 0.05$) on POST 1 day whereas there was no change for sham ($p > 0.05$). For the delta and theta bands (Fig. 3D and G), no significant changes ($p > 0.2$) were observed in the sham or injured groups. In the gamma band (Fig. 3E), mean frequency increased ($p < 0.02$) on POST 1 and 7 days and had no change ($p > 0.05$) on POST 4 day in the sham group; injury caused uniform decreases ($p < 0.0001$). In the sigma frequency (Fig. 3F), mean frequency in the sham group was reduced ($p = 0.004$) on POST 4 days, whereas it increased ($p < 0.0001$) on POST 1 and 4 days in the injured group. There was no change ($p > 0.05$) in sigma mean frequency on POST 7 day for the sham and injury groups. In general, the injury effect magnitude was larger for spectral power than for mean frequency.

Hyperconnectivity in broadband networks during recovery

Global resting state functional connectivity in the broadband network in shams was diminished compared with PRE on POST 1, 4, and 7 days (Fig. 4). The majority of the sham group connections were classified as hypoconnected relative to PRE or had POST-PRE edge weight differences ≤ −5 (shown in white). Over the POST days, the sham group had a relatively modest decrease in the number of hypoconnected edges, with 992, 916, and 912 edges on POST 1, 4, and 7 days, respectively. In contrast, the number of hyperconnected edges relative to PRE (POST-PRE edge weight difference ≥5 and shown in dark blue) for sham increased from 0

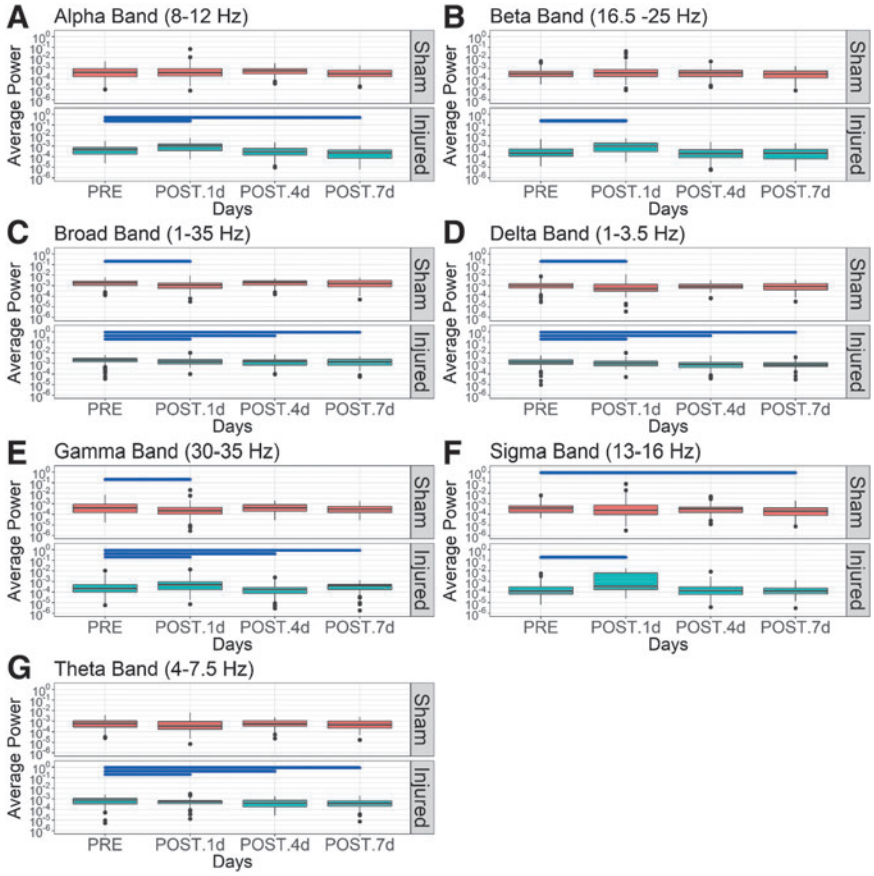

FIG. 2. Box plots of average spectral power (on logarithmic scale) in sham and injured groups on days −1, 1, 4, and 7 across seven frequency bands. A non-parametric Dunnett's test was performed for statistical comparison of post-injury days with pre-injury. Black, horizontal bars indicate significant comparisons ($p < 0.05$).

POST 1 day to 54 and 56 on POST 4 and 7 days, respectively. The injured group had a dramatic transient decrease in the number of hypoconnected edges, with 288, 26, and 2 POST 1, 4, and 7 days respectively. After injury, diffuse hyperconnectivity increased markedly over POST time, with 368, 860, and 964 edges POST 1, 4, and 7 days, respectively. Injury induced a large increase in the number of hyperconnected edges on all POST days, which was more than 10 times the number of hyperconnected edges observed in the sham group. The injured group had substantially fewer hypoconnected edges than sham on all POST days. We performed a non-parametric two sample Wilcox test to compare sham and injured connections at each time point. Sham was significantly different from injured connections at each study day ($p \leq 0.0001$). The differences observed between both groups at PRE are the result of intra-animal variability in this small sample. When subtracting each animal's PRE baseline from the POST measurements, statistically significant differences emerge between injured and sham groups.

Table 1. Percent Change in Average Power Compared with Pre-Levels Were Analyzed at All Frequency Bands, and Averaged across Animals

		Sham			*Injured*		
Average power	*Frequency*	*1 day*	*4 days*	*7 days*	*1 day*	*4 days*	*7 days*
	Alpha (8 1–2 Hz)	0.00%	0.00%	0.00%	*106.78%*	0.00%	**−48.24%**
	Beta (16.5–25 Hz)	0.00%	0.00%	0.00%	*236.69%*	0.00%	0.00%
	Broad (1–35 Hz)	**−26.39%**	0.00%	0.00%	**−15.83%**	**−33.19%**	**−27.59%**
	Delta (1–3.5 Hz)	*0.68%*	0.00%	0.00%	**−11.69%**	**−32.76%**	**−38.25%**
	Gamma (30–35 Hz)	**−3.55%**	0.00%	0.00%	*104.39%*	**−58.58%**	**−33.32%**
	Sigma (13–16 Hz)	0.00%	0.00%	**−50.61%**	*712.77%*	0.00%	0.00%
	Theta (4–7.5 Hz)	0.00%	0.00%	0.00%	**−25.59%**	**−39.13%**	**−40.12%**

Percent change in each metric indicates significant ($p < 0.05$) non-parametric Dunnett's test, where positive changes are shown in italic and negative changes are shown in boldface. Changes that did not reach significance are indicated by 0.00% in regular type.

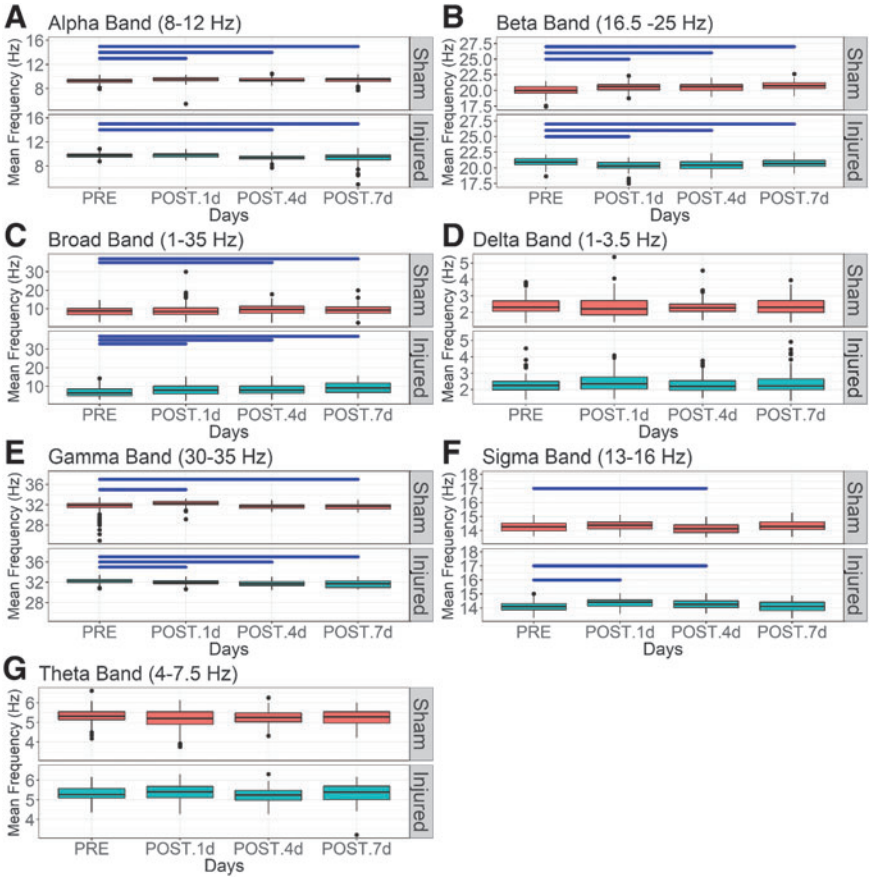

FIG. 3. Boxplots of mean frequency in sham and injured groups on days −1, 1, 4, and 7 across frequency bands, **(A)** alpha, **(B)** beta, **(C)** broad, **(D)** delta, **(E)** gamma, **(F)** sigma, and **(G)** theta. A non-parametric Dunnett's test was performed for statistical comparison of post-injury days with pre-injury. Black horizontal bars indicate significant comparisons ($p < 0.05$).

Effect of TBI on network properties from all analyzed frequency bands

Nodal strength. First, nodal strength quantifies the number and strength of connection that each electrode has to all other electrodes, where a higher nodal strength represents increased synchrony of EEG signals with other electrodes. Shams had reduced ($p < 0.0001$) nodal strength values for alpha networks on POST 1, 4, and 7 days compared with PRE (Table 3, Fig. S1.1). The injured group nodal strength was not significantly different ($p > 0.11$) on any POST days relative to PRE in the alpha band networks. On all POST days, shams had smaller ($p < 0.0001$) beta band nodal strength values, whereas the injured group presented elevated ($p < 0.0001$) beta nodal strength values on POST 1 and 7 days compared with PRE; no change ($p > 0.05$) was observed POST 4 day. In broadband networks, sham showed a decrease ($p < 0.0005$) in nodal strength on POST 1 day, and no change on POST 4 ($p = 0.82$) and 7 days ($p = 0.82$) (Fig. 5A). Broadband network nodal strength from injured animals did not change ($p = 0.1$) on POST 1 day, but showed an increase ($p < 0.0005$)

Table 2. Percent Change in Mean Frequency Compared with Pre-Injury Levels Were Analyzed at All Frequency Bands, and Averaged across Animals

		Sham			*Injured*		
Mean frequency	*Frequency*	*1 day*	*4 days*	*7 days*	*1 day*	*4 days*	*7 days*
	Alpha (8–12 Hz)	*2.57%*	*1.66%*	*1.26%*	0.00%	**−3.66%**	**−3.95%**
	Beta (16.5–25 Hz)	*2.49%*	*2.61%*	*3.50%*	**−2.88%**	**−2.51%**	**−1.25%**
	Broad (1–35 Hz)	0.00%	*11.45%*	*11.07*	*15.50*	*18.97%*	*32.40%*
	Delta (1–3.5 Hz)	0.00%	0.00%	0.00%	0.00%	0.00%	0.00%
	Gamma (30–35 Hz)	*2.19%*	0.00%	*0.21%*	**−.70%**	**−1.50%**	**−1.61%**
	Sigma (13–16 Hz)	0.00%	**−1.01%**	0.00%	*1.82%*	*1.25%*	0.00%
	Theta (4–7.5 Hz)	0.00%	0.00%	0.00%	0.00%	0.00%	0.00%

Percent change in each metric indicates significant ($p < 0.05$) non-parametric Dunnett's test, where positive changes are shown in italic and negative changes are shown in boldface. Changes that did not reach significance are indicated by 0.00% in regular type.

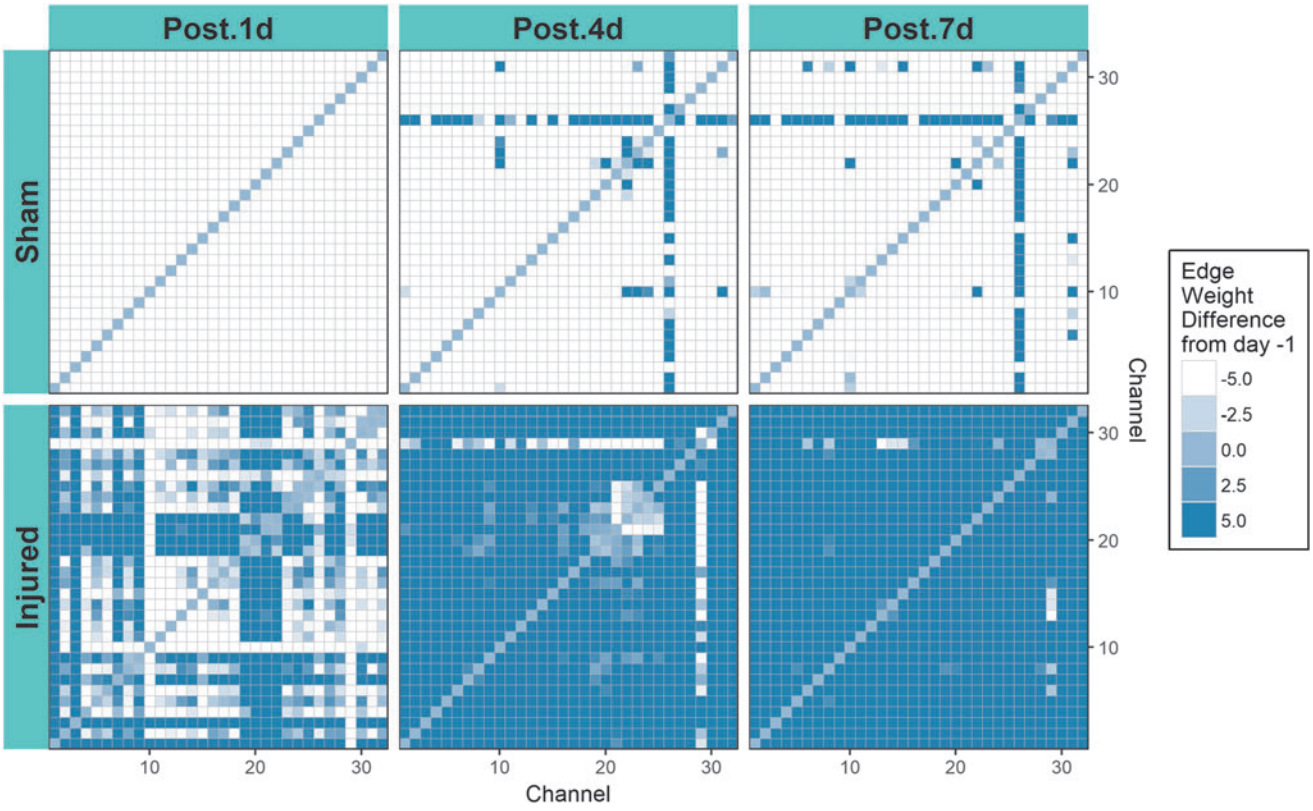

FIG. 4. Broadband network matrices for sham and injured groups showing median differences in edge weight after anesthesia or injury for all piglets. Each matrix shows the difference in connections among 32 electrodes across the piglet brain. The median difference in edge weights was calculated as post-injury–pre-injury across all animals.

on POST 4 and 7 days when compared with PRE. Sham delta band network nodal strength values decreased ($p < 0.0001$) on POST 1 d relative to PRE and had no changeon POST 4 and 7 days; in contrast, the nodal strength values from the injury group were not different ($p > 0.05$) from PRE on POST 1 day but were elevated ($p < 0.0001$) on POST 4 and 7 days. There were significant changes in gamma network nodal strength for sham and injured on all POST days; the injured group showed uniform increases ($p < 0.0001$) in nodal strength relative to PRE, whereas sham nodal strength decreased ($p < 0.0001$) on POST 1, 4, and 7 days. Sigma nodal strength was reduced on all POST days in the sham group, whereas it increased ($p < 0.05$) in the injured group on POST 1 day and had no change on POST 4 and 7 days. In the shams, theta nodal strength decreased on POST 1, 4, and 7 days and the injured group showed a reduction on POST 1 days ($p < 0.0001$), with no change ($p > 0.3$) on POST 4 and 7 days. Overall, there were widespread 6–30% reductions in nodal strength in sham networks across all frequency bands relative to PRE, whereas there were 7–20% elevations in nodal strength after injury.

Clustering coefficient. Second, clustering coefficient represents local clustering within a network that is measured as the average ''intensity'' of triangles around a node. When the average intensity of triangles around a node is low, the local connections are

TABLE 3. PERCENT CHANGE IN MEAN VALUES OF NODAL STRENGTH COMPARED TO PRE-LEVELS ACROSS ALL ANALYZED FREQUENCY BANDS

		Sham			*Injured*		
Nodal strength	*Frequency*	*1 day*	*4 days*	*7 days*	*1 day*	*4 days*	*7 days*
	Alpha (8–12 Hz)	**−30.89%**	**−8.46%**	**−6.87%**	00.00%	0.00%	0.00%
	Beta (16.5–25 Hz)	**−8.96%**	**−6.85%**	**−6.61%**	*14.34%*	0.00%	*3.59%*
	Broad (1–35 Hz)	**−21.67%**	0.00%	0.00%	0.00%	*7.44%*	*8.81%*
	Delta (1–3.5 Hz)	**−23.94%**	0.00%	0.00%	00.00%	7.85%	8.82%
	Gamma (30–35 Hz)	**−31.26%**	**−9.22%**	**−7.50%**	*11.90%*	*8.87%*	*12.94%*
	Sigma (13–16 Hz)	**−13.07%**	**−10.31%**	**−12.39%**	*21.55%*	0.00%	0.00%
	Theta (4–7.5 Hz)	**−31.72%**	**−7.35%**	**−6.03%**	**−15.27%**	0.00%	0.00%

Percent change in each metric indicates significant ($p < 0.05$) non-parametric Dunnett's test, where positive changes are shown in italic and negative changes are shown in boldface. Changes that did not reach significance are indicated by 0.00% in regular type. Base 10 logarithm was applied to nodal strength before analysis.

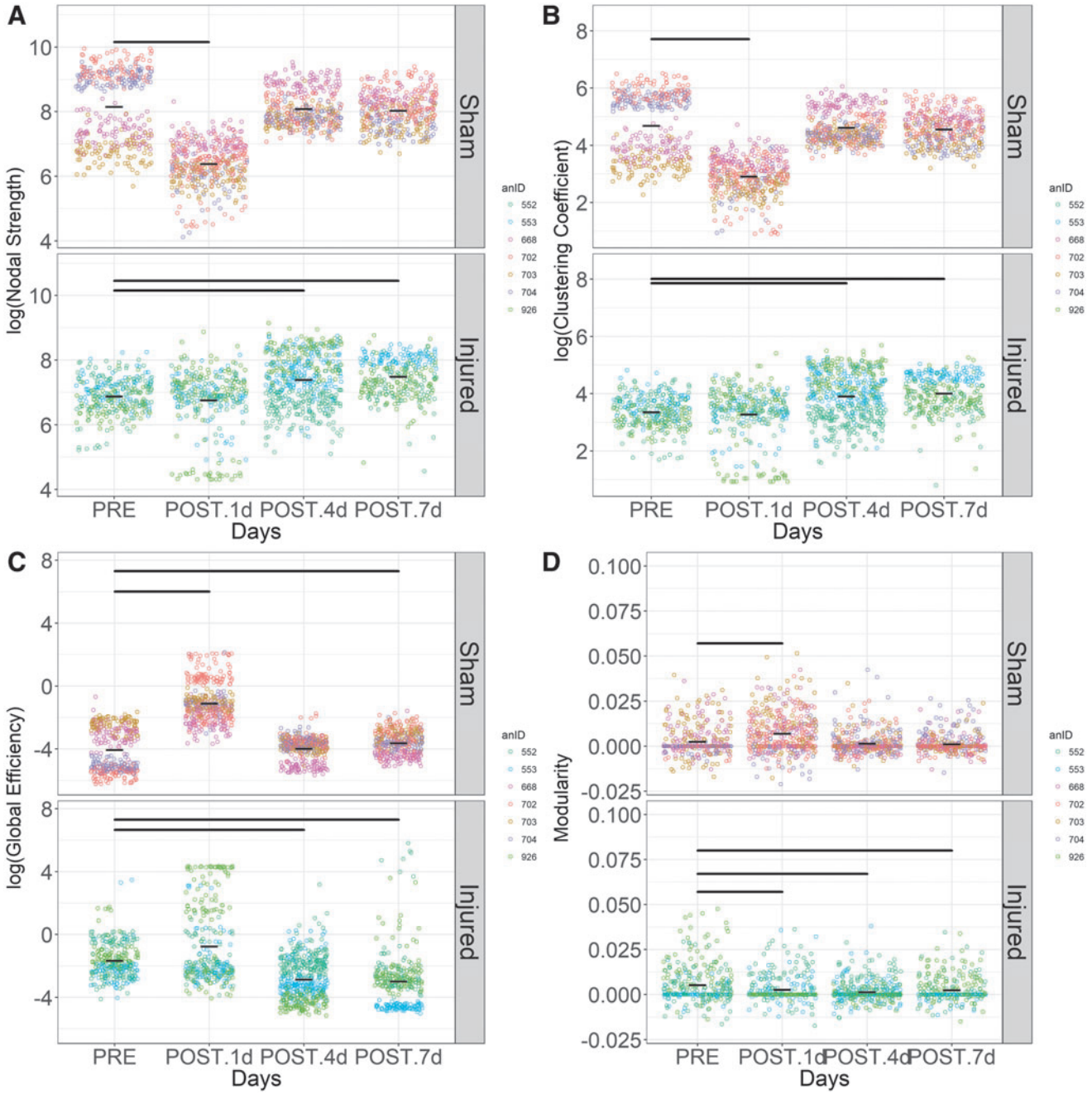

FIG. 5. Comparison of broadband resting state network metrics, **(A)** nodal strength, **(B)** clustering coefficient, **(C)** global efficiency, and **(D)** modularity, by injury group and day. Each open circle represents a single 1 sec, network and each color indicates an animal. The shorter black horizontal bars are mean values over all animals, and the longer black horizontal lines at the top of panels represent significant comparisons of post-injury values relative to pre-injury values using a non-parametric Dunnett's test ($p < 0.05$).

weak. In shams, broadband network clustering coefficient (Fig. 5B) decreased ($p < 0.0005$) on POST 1 day relative to PRE and then returned to PRE values by POST 4 and 7 days ($p = 0.77$); in the injured group, clustering coefficient did not change ($p > 0.05$) on POST 1 day, but it increased ($p < 0.0005$) on POST 4 and 7 days compared with PRE. Clustering coefficient presented the same pattern of changes as nodal strength across all frequency networks and days with much larger changes, where 15–80% reductions were widely observed in the sham group and 16–75% elevations were observed in the injured group (Table 4, Fig. S1.2).

Global efficiency. Third, global efficiency quantifies the functional integration in the brain, which is the ability to rapidly combine specialized information from distributed brain regions. We observed an increase ($p < 0.0005$) in global efficiency from alpha band networks on POST 1 day for both injury and sham groups (Table 5, Fig. S1.3). Global efficiency in shams returned to PRE values by day 4 ($p = 0.35$ and $p = 0.51$ on POST 4 and 7 days, respectively), but remained significantly elevated ($p < 0.0005$) in the injury group on POST 4 and 7 days. Global efficiency in beta band networks for the shams significantly increased ($p < 0.0005$)

Table 4. Percent Change in Mean Values of Clustering Coefficient Compared with Pre-Levels across All Analyzed Frequency Bands

		Sham			*Injured*		
Clustering coefficient	*Frequency*	*1 day*	*4 days*	*7 days*	*1 day*	*4 days*	*7 days*
	Alpha (8–12 Hz)	**−63.78%**	**−17.35%**	**−14.12%**	00.00%	0.00%	0.00%
	Beta (16.5–25 Hz)	**−33.82%**	**−24.15%**	**−23.44%**	*75.06%*	0.00%	*20.28%*
	Broad (1–35 Hz)	**−37.85%**	0.00%	0.00%	0.00%	*16.21%*	*19.37%*
	Delta (1–3.5 Hz)	**−42.57%**	0.00%	0.00%	0.00%	17.54%	20.09%
	Gamma (30–35 Hz)	**−78.90%**	**−23.02%**	**−18.64%**	*69.85%*	*53.92%*	*78.55%*
	Sigma (13–16 Hz)	**−74.52%**	**−54.90%**	**−65.94%**	*320.63%*	0.00%	0.00%
	Theta (4–7.5 Hz)	**−58.94%**	**−13.57%**	**−11.11%**	**−38.47%**	0.00%	0.00%

Percent change in each metric indicates significant ($p < 0.05$) non-parametric Dunnett's test, where positive changes are shown in italic and negative changes are shown in boldface. Changes that did not reach significance are indicated by 0.00% in regular type. Base 10 logarithm was applied to clustering coefficient before analysis.

on POST 1, 4, and 7 days compared with PRE, but did not change in the injured group on any POST day (POST 1 day, $p = 0.055$; POST 4 days, $p = 0.055$; POST 7 days, $p = 0.59$). Sham animals increased in broadband network global efficiency on POST 1 and 7 days ($p < 0.0001$) compared with PRE, but had no change ($p = 0.61$) on POST 4 day (Fig. 5C). In contrast, injured networks had reduced global efficiency values ($p < 0.0001$) at POST 4 and 7 days. Significant elevations ($p < 0.0005$) in delta band global efficiency were observed in sham on all POST days relative to PRE, whereas the injured group had reduced ($p < 0.0001$) global efficiency on POST 4 and 7 days, with the exception of POST 1 day when an increase ($p = 0.045$) was seen. Sham presented increases ($p < 0.02$) in global efficiency in gamma band networks on POST 1 and 4 days, but no change ($p = 0.36$) on POST 7 day. In the injured group, global efficiency increased ($p = 0.004$) on POST 1 day, then decreased ($p = 0.0002$) on POST 4 day before returning to PRE values on POST 7 day ($p > 0.05$). Sigma band networks in the sham group had elevated ($p < 0.001$) global efficiency at POST 1, 4, and 7 days and the injured group had an increase on POST 1 day relative to PRE. Both the injured and sham groups had elevated ($p < 0.0005$) theta network global efficiency values on POST 1 day compared with PRE; however, only the injured group yielded significant increases in global efficiency on POST 4 and 7 days ($p < 0.0005$). Out of all frequency bands, sham presented 6–2103% increases ($p < 0.05$), whereas only the injured group exhibited 71–225% reductions ($p < 0.05$) in global efficiency in the broad, delta, and gamma bands on POST 4 and 7 days relative to PRE.

Modularity. Fourth, modularity measures the degree to which the network organizes its connections into segregated clusters of nodes and edges. For alpha networks, we observed an increase ($p < 0.0001$) and then a decrease ($p < 0.05$) in modularity on POST 1 and 7 days, respectively in the sham group (Table 6, Fig. S1.4). After injury, modularity decreased ($p < 0.04$) on POST 1 and 4 days relative to PRE; no changes ($p = 0.18$) were observed on POST 7 days. Beta network modularity significantly increased ($p < 0.01$) on POST 1, 4, and 7 days, whereas for the injured group, modularity decreased ($p = 0.002$) on POST 7 day relative to PRE. There was an increase ($p < 0.0001$) in broadband network modularity for sham POST 1 day, whereas modularity decreased for the injured group on POST 1 ($p = 0.01$), 4 ($p < 0.0001$), and 7 days ($p = 0.003$) relative to PRE (Fig. 5D). Delta network modularity increased ($p < 0.0001$) on POST 1 day for sham, but decreased ($p < 0.0002$) on POST 4 and 7 days, whereas modularity in the injured group decreased ($p < 0.0001$) on all POST days. Gamma network modularity increased ($p < 0.01$) on POST 1 and 4 days for the shams, whereas in the injured group, modularity decreased ($p < 0.0001$) on POST 4 days after injury. Modularity in the sigma networks increased ($p = 0.04$) on POST 7 day for the shams and decreased ($p = 0.0001$) in the injured group on POST 1 day. In the sham group, increases ($p < 0.05$) were observed in the theta network modularity on POST 1 and 4 days, followed by a reduction ($p = 0.05$) on POST 7 days. Injury resulted in a reduction ($p < 0.0001$) in theta network modularity on POST 4 day compared with PRE. In summary, significant elevations (by 30–564%) were observed on POST 1 day in the sham group across all frequency

Table 5. Percent Change in Mean Values of Global Efficiency Compared with Pre-Levels across All Analyzed Frequency Bands

		Sham			*Injured*		
Global efficiency	*Frequency*	*1 day*	*4 days*	*7 days*	*1 day*	*4 days*	*7 days*
	Alpha (8–12 Hz)	*103.47%*	0.00%	0.00%	231.55%	13.13%	50.75%
	Beta (16.5–25 Hz)	*171.47%*	*8.62%*	*6.76%*	0.00%	0.00%	0.00%
	Broad (1–35 Hz)	*73.05%*	0.00%	*10.80%*	0.00%	**−71.75%**	**−79.16%**
	Delta (1–3.5 Hz)	*92.90%*	*5.84%*	*11.70%*	*1.71%*	**−86.40%**	**−122.12%**
	Gamma (30–35 Hz)	*137.86%*	*9.48%*	0.00%	*199.47%*	**−225.76%**	0.00%
	Sigma (13–16 Hz)	*2103.46%*	*346.17%*	*460.88%*	*51.08%*	0.00%	0.00%
	Theta (4–7.5 Hz)	*89.70%*	0.00%	0.00%	*153.20%*	*10.66%*	*30.00%*

Percent change in each metric indicates significant ($p < 0.05$) non-parametric Dunnett's test, where positive changes are shown in italic and negative changes are shown in boldface. Changes that did not reach significance are indicated by 0.00% in regular type. Base 10 logarithm was applied to global efficiency before analysis.

Table 6. Percent Change in Mean Values of Modularity Compared with Pre-Levels across All Analyzed Frequency Bands

		Sham			*Injured*		
Modularity	*Frequency*	*1 day*	*4 days*	*7 days*	*1 day*	*4 days*	*7 days*
	Alpha (8–12 Hz)	*172.83%*	0.00%	**−54.42%**	**−29.58%**	**−37.35%**	0.00%
	Beta (16.5–25 Hz)	*30.91%*	*53.95%*	*34.04%*	0.00%	0.00%	**−41.49%**
	Broad (1–35 Hz)	*175.13%*	0.00%	0.00%	**−47.10%**	**−73.14%**	**−51.91%**
	Delta (1–3.5 Hz)	*90.34%*	**−86.41%**	**85.17%**	**−37.41%**	**−87.53%**	**−62.62%**
	Gamma (30–35 Hz)	*120.87%*	*14.83%*	0.00%	0.00%	**−33.77%**	0.00%
	Sigma (13–16 Hz)	0.00%	0.00%	*32.20%*	**−45.68%**	0.00%	0.00%
	Theta (4–7.5 Hz)	*564.74%*	*27.29%*	**−56.17%**	0.00%	**−36.84%**	0.00%

Percent change in each metric indicates significant ($p < 0.05$) non-parametric Dunnett's test, where positive changes are shown in italic and negative changes are shown in boldface. Changes that did not reach significance are indicated by 0.00% in regular type.

bands, whereas decreases (by 29–87%) or no changes in modularity were seen in the injured group on POST 1, 4, and 7 days.

We used standard deviation (SD) for each network metric, frequency band, and day to quantify session (day-to-day) variability across animals, because SD provides a reliable measure of the spread of the distribution of each animal's metric. A two way analysis of variance (ANOVA) with repeated measures (to account for multiple measures from the same animal) was performed on the SD values by day and frequency band separately for the sham ($p = 0.5$) and injured groups. Nodal strength variability was not affected by day in the sham or injured ($p = 0.291$) groups. For clustering coefficient, variability was not significantly affected by day in the sham ($p = 0.513$) or injured group ($p = 0.297$). There was no effect of days on global efficiency SD in the sham ($p = 0.091$) or injured ($p = 0.31$) group. For modularity, there was no effect of days on variability for the sham ($p = 0.145$) or injured ($p = 0.534$) group. The variability of all metrics was significantly affected ($p < 0.01$) by frequency band in both the sham and injured groups. Day-to-day variability across animals did not significantly affect any network metric; however, it was affected by frequency band.

In the injured group, alpha band nodal strength and clustering coefficient did not significantly change on 1, 4, or 7 days post-injury relative to PRE, whereas in the sham group nodal strength decreased on all days. Alpha band global efficiency increased on POST 1 day in the sham and injured groups, but presented no significant change at POST 4 and 7 days in the sham. whereas increases were found in the injured group relative to PRE. An increase in alpha modularity was seen on 1 day post-anesthesia, then no change and a decrease at POST 4 and 7 days, respectively, in the sham group. Modularity decreased on POST 1 and 4 days, but returned to pre-injury levels by POST 7 day for the injured group.

For the beta frequency band, nodal strength and clustering coefficient were reduced on all post-anesthesia days relative to PRE in the sham group, but increased on POST 1 and 7 days in the injured group; no change was observed on POST 4 day. Global efficiency in the beta band increased in the sham group and did not change in the injured group for all post-injury days. Beta modularity increased on POST 1, 4, and 7 days in the sham group relative to PRE; however, in the injured group, modularity did not vary from pre-injury levels on POST 1 and 4 days and then decreased on POST 7 day.

Broad and delta band nodal strength and clustering coefficient decreased on POST 1 day in the sham group and then returned to pre-anesthesia levels. In contrast, the injured group had pre-injury levels of nodal strength and clustering coefficient on POST 1 day and then increased 4 and 7 days post-injury. Broad and delta global efficiency had increases on all post-anesthesia days in the sham group, whereas in the injured group it increased on POST 1 day then decreased on POST 4 and 7 days. Broad and delta band modularity increased on POST 1 day in the sham group and then decreased or did not change on POST 4 and 7 days, whereas the modularity decreased on all post-injury days in the injured group.

Gamma nodal strength and clustering coefficient decreased on all post-anesthesia days in the sham group and then increased on all post-injury days in the injured group. Gamma global efficiency increased on POST 1 and 4 days and then returned to PRE levels on POST 7 day in the sham group, whereas global efficiency increased on POST 1 day and then decreased on POST 4 day before returning to pre-injury levels on POST 7 day in the injured group. In the sham group, gamma modularity increased on POST 1 and 4 days before returning to PRE levels, whereas in the injured group, modularity did not vary from PRE levels on POST 1 and 7 days but did decrease on day 4 post-injury.

Nodal strength and clustering coefficient in the sigma band decreased on all post-anesthesia days for the sham group and increased on POST 1 day then returning to PRE levels in the injured group. Sigma global efficiency increased on all POST days in the sham group, but only increased 1 day post-injury before returning to pre-injury levels on POST 4 and 7 days. Sigma modularity stayed at PRE levels on POST 1 and 4 days and then increased at POST 7 day in the sham group, whereas modularity decreased on POST 1 day and then returned to PRE levels on 4 and 7 days post-injury in the injured group.

In the sham group, theta nodal strength and clustering coefficient decreased on 1, 4 and 7 days post-anesthesia, whereas in the injured group it decreased on 1 day post-injury then returned to PRE levels on POST 4 and 7 days. Theta global efficiency increased on POST 1 day and then returned to PRE levels on POST 4 and 7 days in the sham group; global efficiency in the injured group increased on 1,4, and 7 days post-injury relative to PRE. Modularity in the theta band increased on 1 and 4 days post-anesthesia then decreased on POST 7 day in the sham group, whereas modularity did not vary from PRE levels on POST 1 and 7 days and decreased on POST 4 day in the injured group.

On post-injury day 1, nodal strength and clustering coefficient did not change from pre-injury levels in the alpha, broad, and delta bands; increased in the beta, gamma, and sigma bands; and decreased in the theta band. Global efficiency increased in the alpha, delta, gamma, sigma, and theta bands and did not change from PRE

levels in the beta and broad bands on post-injury day 1. Modularity in the inured group decreased in the alpha, broad, delta, and sigma bands and did not change in the beta, gamma, and theta bands.

Nodal strength and clustering coefficient in the injured group increased in the broad, delta, and gamma bands at 4 days post-injury, whereas they did not significantly vary from PRE levels in the alpha, beta, sigma, and theta bands. Global efficiency increased in the alpha and theta bands; decreased in the broad, delta, and gamma bands; and did not change from PRE levels in the beta and sigma bands at 4 days post-injury. At 4 days post-injury, modularity decreased in the alpha, broad, delta, gamma and theta bands, and did not change in the beta and sigma bands.

At 7 days post-injury, nodal strength and clustering coefficient increased in the beta, broad, delta, and gamma bands, whereas they did not change from PRE levels in the alpha, sigma, and theta bands. Increases in global efficiency were found in the alpha and theta bands, decreases were found in the broad and delta bands, and no changes were found in the beta, gamma, and sigma bands at 7 days post-injury. Modularity decreased in the beta, broad, and delta bands and did not change in the alpha, gamma, sigma, and theta bands.

Core network topology across frequency bands

For every animal, the core network topology or arrangement of edges was calculated as the 95th percentile of the sum of all statistically significant 1 sec binary networks over the entire duration of the EEG recording. The core edges represent the strongest connections throughout the brain in a given frequency band before and after TBI. Visual inspection of each piglet's topology across all analyzed frequencies (Fig. S 2.1–2.7) showed that the arrangement of edges between the sham and injured groups did not differ. There was remarkably consistent alpha band network topology (averaged over all pigs) before and after injury (Fig. 6). The number of edges present in the core topology was also consistent among animals and on different days. The alpha band core topology had several edges in the left and frontal regions of the brain. We observed similar conservation of core network topology before and after TBI in the beta band, but with distinct signature configurations (Fig. 7) of core edges that were symmetrical around the midline. The averaged broadband core topology was similar in the sham and injured groups, with edges that were slightly more focused in the right hemisphere and across the frontal, temporal, and parietal nodes (Fig. 8). Averaged delta core edges were similar in the sham and injured groups and focused in the right, occipital region (Fig. 9). Averaged gamma core networks had the majority of edges in the right hemisphere (Fig. 10) in both the sham and injured groups. Averaged sigma core networks were similar in the sham and injured groups with symmetrical distribution around midline and in all regions (Fig. 11). Theta edges were focused in the left hemisphere (Fig. 12) for both the sham and injured groups. The total number and arrangement of core edges were dependent on the frequency band of interest, but did not change with injury or study day.

Discussion

''Resting state'' typically involves subjects sitting with eyes closed in a dark room while awake and free from any overt stimuli. Resting state EEG data acquisition is easier to collect and simpler for the subject than task-based procedures, which is appealing to

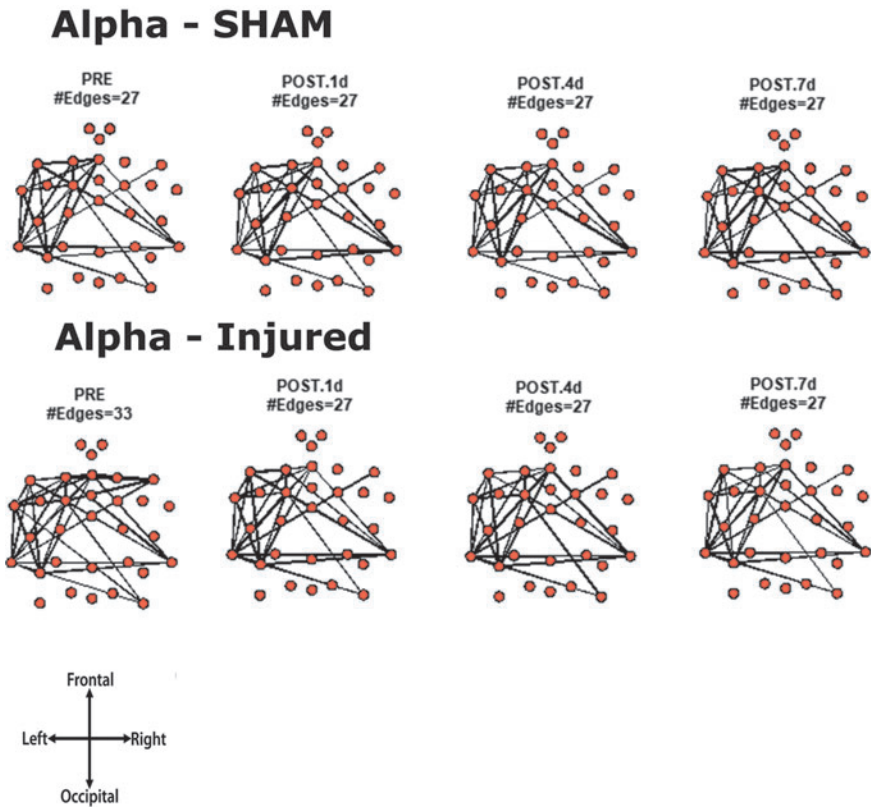

FIG. 6. Averaged (across all piglets) core alpha band networks with the most consistent edges (95th percentile of frequency over the sum of 88 1 sec networks) from sham and injured groups.

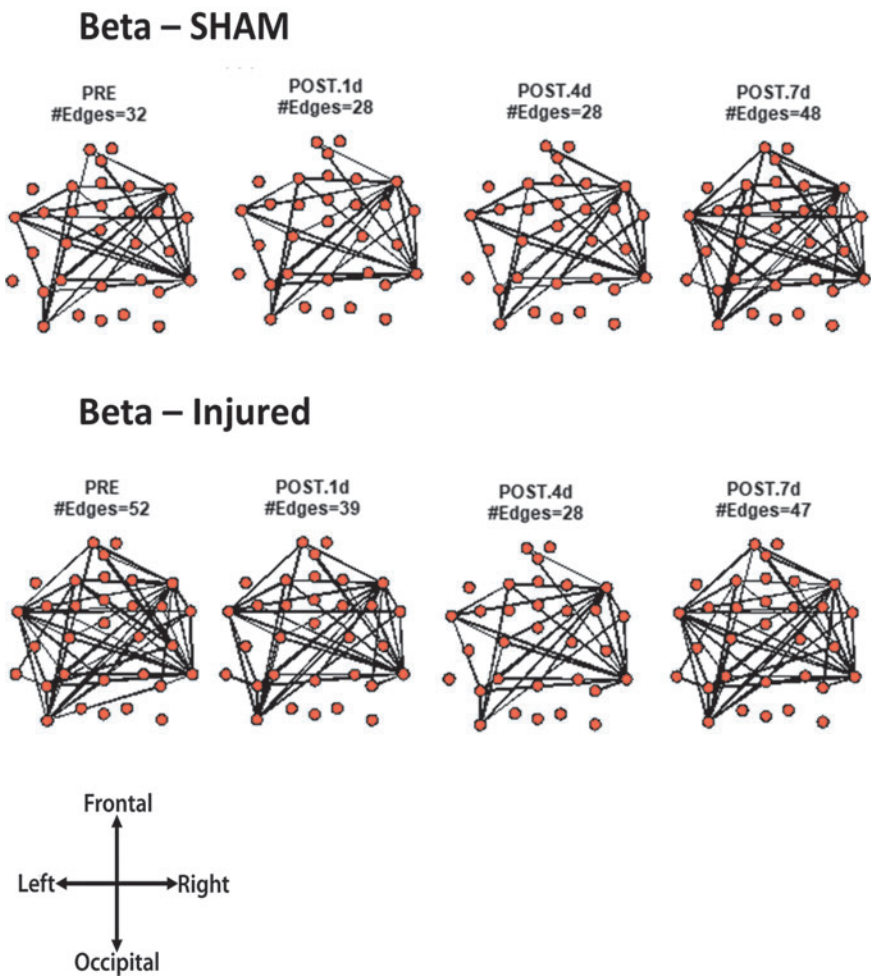

FIG. 7. Averaged (across all piglets) core beta band networks with the most consistent edges (95th percentile of frequency over the sum of 88 1 sec networks) from sham and injured groups.

the study of pediatric populations, for whom cognitive tasks can be more difficult or frustrating in unpredictable ways. However, identification of abnormalities in EEG recordings after mTBI can be subtle compared with controls, and may be subject to bias by the interpreter. Although there are several resting state functional MRI (fMRI) studies in adults that report both increases and decreases in functional connectivity after TBI,[45–50] hyperconnectivity was reported by the only resting state fMRI study on a pediatric TBI cohort.[51] Virji-Babul and colleagues reported increased local connectivity, but no change in global connectivity of resting state EEG networks in adolescent athletes with a sports-related concussion.[52] There is a small number of resting state EEG studies of TBI in adults;[53] however, there are no reports on pediatric EEG functional networks following TBI. This report fills the gap in the TBI resting state EEG literature by studying the effect of diffuse TBI in piglets. We hypothesized that TBI would induce acute and chronic changes in the properties of resting state EEG functional networks that were also dependent on the frequency band of interest.

TBI changes spectral power and mean frequency for different frequency bands

We observed lower spectral power and reduction in frequency in the alpha and beta bands in our piglets 4 and 7 days following injury, and this change was absent in shams. The suppression of alpha spectral power may imply balance dysfunction.[54] Reductions in alpha and beta amplitudes have been associated with diminished cognitive function.[55] Mild, diffuse reduction in the alpha band mean frequency is a common EEG abnormality that is observed in TBI patients.[6,56–59] Tebano and colleagues reported reductions of fast beta (20–35 Hz) mean frequency 3–10 days following mTBI compared with normal controls.[58] Their fast beta range corresponds to a portion of the beta (16.5–25) and gamma (30–35 Hz) bands used in this report. In our study, a significant change in mean theta frequency was not observed, which aligns with previously published studies that report inconsistent changes in the theta band in TBI patients.[56,58] We saw no significant changes in the delta mean frequencies post-injury in our piglets, in contrast to the increases[60–63] and decreases[64] that have been observed in TBI patients during post-injury hours to weeks. In our study, we observed decreases in delta and theta average spectral power. Increased theta and delta power may be associated with postural instability.[65]

When the brain engages in certain functions, such as directing attention or processing sensory stimuli, select oscillations are dominant.[66] Theta and gamma activity are prominent in locomotion. Theta oscillations are linked to memory functions in the hippocampus. Delta oscillations appear to be implicated in many cognitive processes such as autonomic functions, high emotional

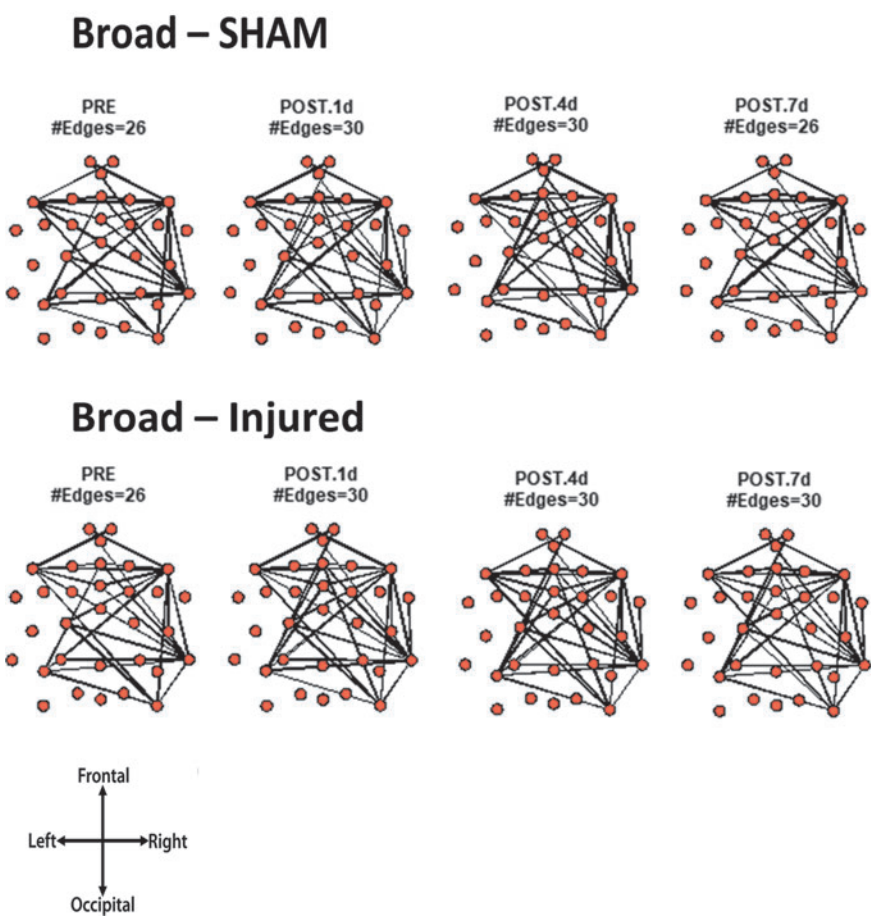

FIG. 8. Averaged (across all piglets) core broadband networks with the most consistent edges (95th percentile of frequency over the sum of 88 1 sec networks) from sham and injured groups.

involvement and behavioral inhibition.[67] Slow oscillations may involve many neurons in large brain areas, whereas the brief time intervals of fast oscillations facilitate local integration because of limits of axon conduction delays. If an axon's myelin sheath is damaged, this may lead to increased axonal conduction delays and subsequent increased power in slow oscillation ranges. There is much less research on delta and beta range rhythms in infants and young children.[37] Alpha rhythm emerges at approximately 3 months of age and is sensitive to visual input: it increases in amplitude when the eyes are closed.[37] Alpha is implicated in visual attention and processing. Theta oscillations are often observed during the transition from wakefulness to sleep in adults. An increase in theta power has been associated with processing of emotional information and memory-related tasks. In infants, an increase in theta power has been linked to executive control of attention. Studies of the gamma rhythm in infants and adults report its relation to active memory retrieval, where familiar stimuli evoke a greater gamma band response than do unfamiliar stimuli.[37]

Oscillatory activity contributes to higher order information processing; for example, hippocampal theta (3–12 Hz) oscillations are concurrent with spatial learning deficits.[68,69] Hippocampal interneurons are vulnerable to cell death and altered function after TBI, which may contribute to the changes observed in the theta band. Following injury in rodents, there is a decrease in alpha, beta, delta, and theta power.[70–73] Slower oscillatory rhythms can reset and bias computation in multiple cortical regions.[66] Changes in EEG are observed in the alpha, beta, delta, theta, and gamma bands and are not state dependent because alterations are noted when a patient is at rest,[52,74] actively moving,[54] or asleep.[75,76] The changes in average power and mean frequency from the alpha and beta bands induced by TBI in our piglets were generally consistent with findings reported in TBI patients, providing the basis for applying network analysis to our EEG data. Several studies that report hyperconnectivity following brain trauma speculate on its mechanisms. Nakamura and colleagues[77] suggest that the increase in neural connections signifies an increase in the utilization of auxiliary resources, which later subsides and results in a more efficient neural network. Stevens and colleagues[78] report that the enhanced connectivity may be the result of compensatory processes in the form of enhanced task-specific processing such as visual or limbic activity. They also cited the work of Sharp and colleagues[50] that interpreted hyperconnectivity as the result of the brain's reduced capacity to maintain neural activation profiles. Namely, diffuse neuronal impairment may cause compensatory alterations to the responsiveness of the entire network to more efficiently mediate behavior. Friston and colleagues[79] reported that enhanced brain activity across distant brain regions may indicate that these regions communicate via excitatory pathways. The EEG frequency bands represent different oscillatory phenomena that may be the result of intrinsic neuronal characteristics, corticocortical connections, and/or thalamocortical connections. TBI may cause changes to selective neuronal populations and excitatory, cortical connections

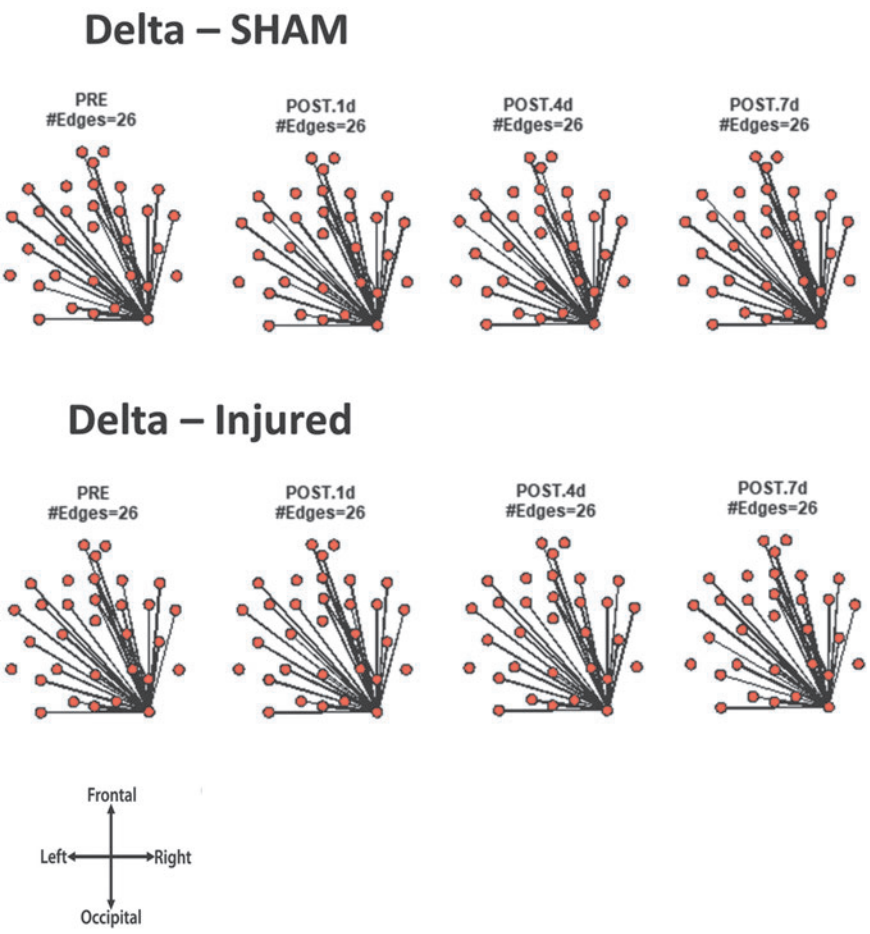

FIG. 9. Averaged (across all piglets) core delta band networks with the most consistent edges (95th percentile of frequency over the sum of 88 1 sec networks) from sham and injured groups.

that result in the simultaneous increase in functional hyperconnectivity and a decrease in the power of the lower EEG frequencies. Future studies should explore the relationship between functional connections across the young brain and the pathophysiological basis for oscillations in the EEG frequency bands after TBI.

TBI affects resting state EEG network metrics in all analyzed frequency bands

The resting state network represents the synchrony of background EEG activity across the brain. We observed changes in nodal strength, clustering coefficient, global efficiency, and modularity within the same animal on a single day as a result of the rapidly changing dynamics of neural activity on the time scale of seconds; this was comparable to previously published studies.[36,38] Specifics are described subsequently. Additionally, we also observed changes in network metrics between sham and injured subjects; changes there were dependent on the frequency band of interest. Whereas alterations in average power and mean frequency were frequency band dependent, only changes in global efficiency were influenced by frequency band. There were significant changes in several resting state network metrics in the traumatic brain injured (sagittal rapid head rotation) group that were not observed in the shams. After TBI, there were reductions in modularity as well as elevations in nodal strength and clustering coefficient across all analyzed frequencies.

Nodal strength and clustering coefficient both increased in the beta, broad, delta, gamma, and sigma bands as they both capture the heightened global and local connectivity throughout the brain. In contrast, we found that after TBI, alpha network connectivity did not change relative to pre-injury and that the theta network connectivity decreased at 1 day post-injury. Several studies report hyperconnectivity in resting state networks like that observed in the beta, broad, delta, gamma, and sigma bands. Resting state fMRI connectivity was elevated in children with mild to moderate TBI.[51] Several resting state studies in adults report hyperconnectivity after TBI using fMRI[45,80,81] and EEG networks.[53,82] Sharp and colleagues reported overall increased default mode network connectivity in moderate/severe TBI patients with cognitive impairment 6 months after injury.[50] Porter and colleagues[53] reported hyperconnectivity in the right inferior frontal gyrus, and hypoconnectivity in the left inferior frontal gyrus in the chronic TBI group relative to controls, calculated from resting state EEG recordings. An increase in local clustering was observed in adult rats at 7 days following mild and moderate controlled cortical impact (CCI) injuries relative to pre-injury,[83] which was similar to the current study findings of increases in nodal strength and clustering coefficient at 7 days in the beta, broad, delta, and gamma bands. Hyperconnectivity in EEG and fMRI resting state networks is

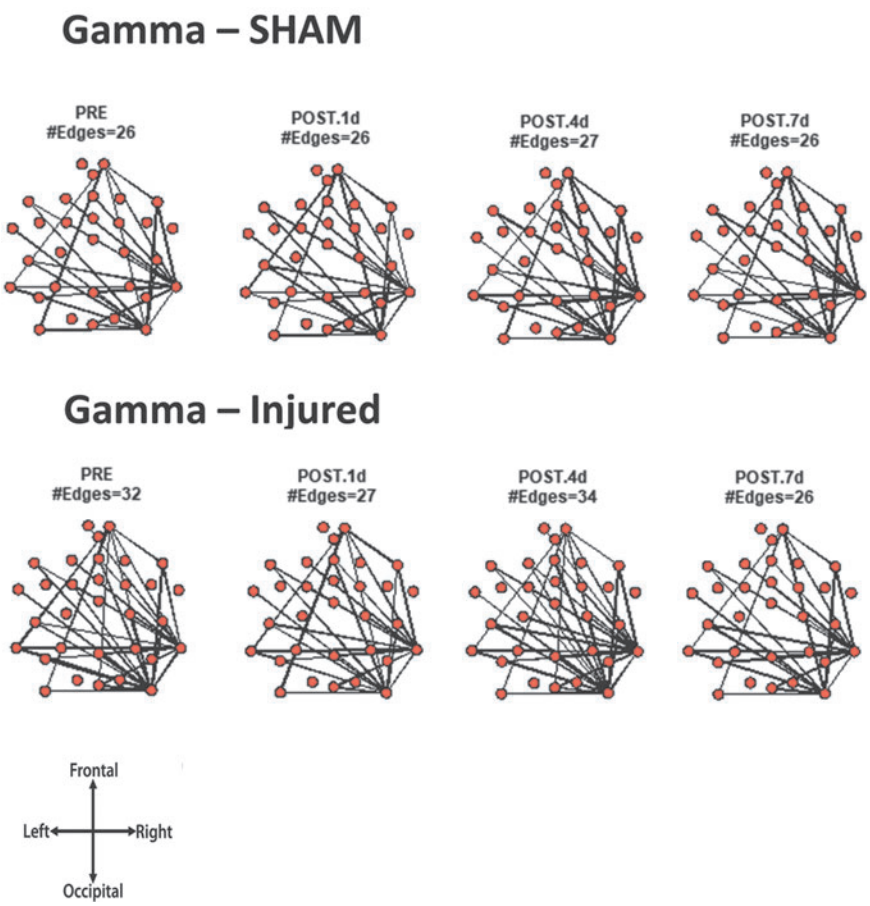

FIG. 10. Averaged (across all piglets) core gamma band networks with the most consistent edges (95th percentile of frequency over the sum of 88 1 sec networks) from sham and injured groups.

evident after injury in children, adults and rats for various TBI severities and recovery durations. In summary, our studies are in agreement with the resting state literature, in which hyperconnectivity is observed following TBI.

Despite the prevalence of reports of hyperconnectivity in resting state functional networks after trauma, it is important to note that some studies report hypoconnectivity following TBI.[48,49,78,84] Stevens and colleagues[78] reported region-dependent changes in resting state (fMRI blood-oxygen-level dependent [BOLD]) functional connectivity in an mTBI cohort relative to age-matched controls. Palacios and colleagues[48] reported region-dependent alterations in resting state functional connectivity at 6 months after injury in a large and clinically well-defined mTBI sample. Our study found hypoconnectivity only in the theta band at 1 day post-injury; however, without a more chronic time point (e.g., 1 month post-injury) it is challenging to compare across studies. Mishra and colleagues[84] reported lower resting fMRI correlation coefficients between the ipsilateral parietal cortex and ipsilateral hippocampus in adult rats 4 months following TBI compared with shams.[84] Mishra's findings disagreed with our findings of hyperconnectivity after injury in the beta, broad, delta, gamma, and sigma bands; however, differences may be attributed to the scanning being performed while the rat was under anesthesia, which may affect brain activity. We speculate that the brain region or the source of neural activity and its dominant frequency influences the extent of synchrony across cortical neuronal clusters. Virji-Babul and colleagues found that concussion in adolescent athletes did not alter resting state EEG global network efficiency, modularity, or clustering coefficient,[52] whereas our study found significant changes in all metrics and frequency bands. We found variable frequency-specific changes in global efficiency after injury. In alpha, beta, sigma, and theta networks, global efficiency either increased or did not change post-injury, generally in contrast to increases observed in shams on the same day. For the broad, delta, and gamma bands, reductions in global efficiency were observed for injured animals. In a study of sedated adult rats, post-CCI fMRI network global efficiency increased compared with pre-injury,[83] Harris's findings agreed with our findings in the alpha, delta, gamma, sigma, and theta bands at 1 day post-injury. The lack of anesthesia during EEG acquisition in our study may explain the opposite polarities of change in global efficiency in the broad, delta, and gamma bands at 4 and 7 days post-injury. The reduction in global efficiency may indicate loss of neural computational ability, perhaps as a result of decreases in efficient communication throughout the network. The contrasting direction of change between injured and sham groups makes global efficiency a candidate metric for identifying injured networks and for measuring recovery from TBI.

Following injury, we report that modularity across all analyzed frequency bands decreased or did not change, which was generally distinct from changes observed in same-day shams. After injury, there was a lower degree of segregation of the brain into smaller functional units. Similarly, a resting-state fMRI BOLD contrast imaging study in adult rats found a significant decrease in modularity 7 days after CCI injury.[83] Han and colleagues reported an

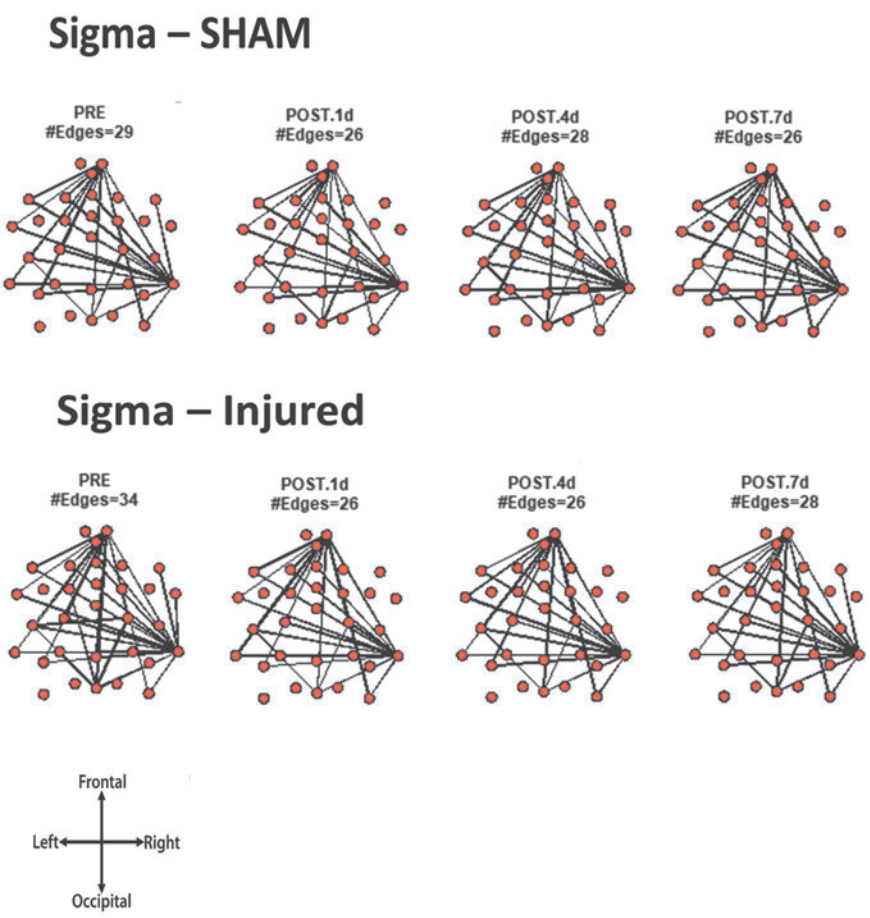

FIG. 11. Averaged (across all piglets) core sigma band networks with the most consistent edges (95th percentile of frequency over the sum of 88 1 sec networks) from sham and injured groups.

increase in modularity of resting state functional connectivity in an adult TBI cohort at 90 days post-blast compared with healthy controls. However, no change was observed 6–12 months after the initial scan.[85] We speculate that a damaged brain network is less modular because more connections form between previously defined functional modules. The reduction in functional segregation across the network implies a breakdown of information encapsulation among specialized brain systems, which may be associated with functional and cognitive deficits.[86]

Synchrony among EEG signals from different frequency bands implies specialized neural communication, plasticity, formation of functional ensembles, and consolidation of long-term memories. Temporal synchronization may also be important in information binding and computing in the brain. Hyperconnectivity may depend on demand and resource availability. We found increased synchrony in the beta, broad, delta, gamma, and sigma frequency bands after TBI, which may be related to dysfunctional cortical activity. Several studies demonstrate that TBI alters physiological oscillatory rhythms.[68,69,87] Increased connectivity was observed following TBI.[81] Luo and colleagues found abnormality in the delta (1–4 Hz) frequency band of resting state magnetoencephalography (MEG) signals in military veterans ≥6 months after mTBI compared with healthy controls.[88] Douw and colleagues reported that better cognitive performance correlated with increased local connectivity of MEG functional networks in the theta band and higher clustering coefficient in the delta and theta bands.[89] The hyperconnectivity of EEG functional networks could play a crucial role in the monitoring of cognitive function before and after TBI-induced change in oscillations, which can impact behavioral function.

EEG recordings may be influenced by anesthesia drugs[31–33] such as isoflurane, which has a varied effect on cerebral metabolic rate and cerebral blood flow (CBF) in adults[90–94] and children.[95] Isoflurane improved functional outcome and attenuated Cornu Ammonis (CA)1 damage compared with fentanyl treatment post-TBI. Isoflurane may be neuroprotective by augmenting CBF, improving motor function, and reducing excitotoxicity after TBI.[96,97] Isoflurane has been reported to induce neurodegeneration via increased numbers of apoptotic cells 4 and 48 h after CCI in adult rats.[98] Isoflurane was shown to affect motor function in rats 1–5 days after exposure compared with the pre-injury time point.[97] Anesthesia was administered to all piglets studied shortly before injury and to shams, and may have considerable (acute and chronic) impact on the resting-state EEG network metrics and axonal injury following TBI. Baseline cerebral perfusion pressure was lower after isoflurane was administered compared with total IV anesthesia in immature (4 week) uninjured pigs, which may suggest reduced autoregulation.[99,100] Isoflurane was also shown to increase cerebral blood volume and CBF in uninjured rats compared with propofol or pentobarbital.[92] Kochs and colleagues demonstrated that 1% isoflurane led to a shift toward slower EEG frequencies in uninjured dogs within 90 min.[93] The cerebrovascular and cerebral

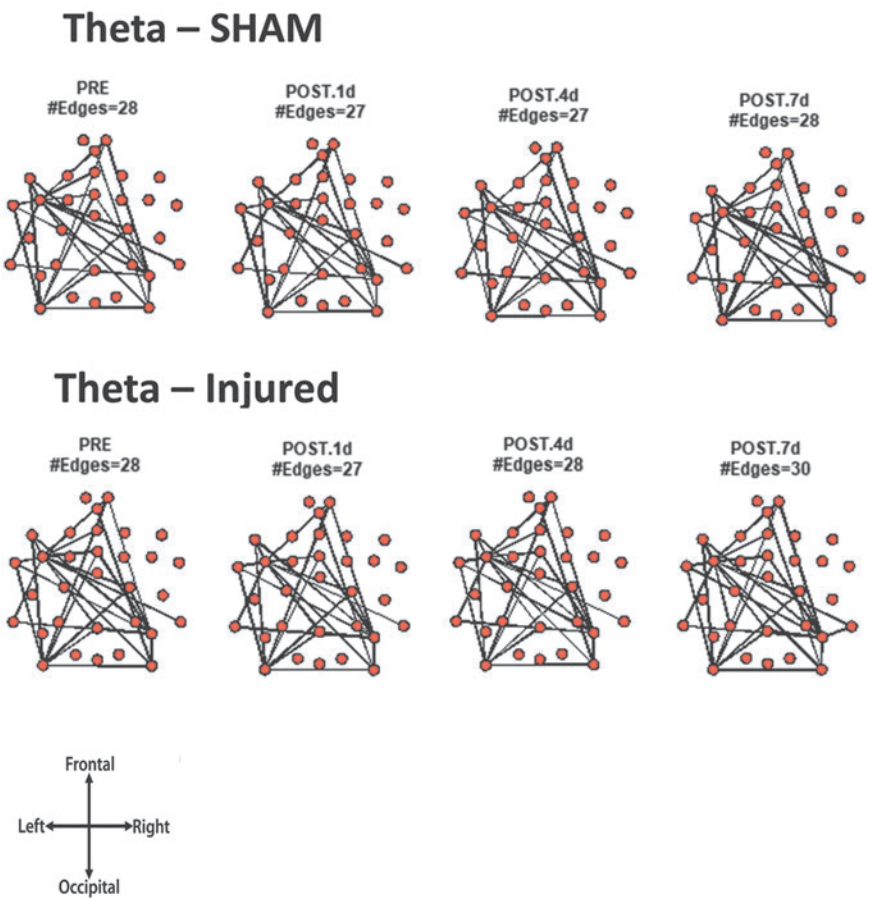

FIG. 12. Averaged (across all piglets) core theta band networks with most the consistent edges (95th percentile of frequency over the sum of 88 1 sec networks) from sham and injured groups.

metabolic effect of anesthesia may explain the difference observed between the pre and post-TBI resting state EEG network metrics in the sham group.

Our TBI model in 4-week-old piglets has been shown to produce consistent behavioral outcomes for the head velocity ranges and head rotation directions used in this article.[101–104] Sagittal rotations in 4-week-old piglets led to increased behavioral deficits, axonal injury, and CBF deficits in comparison with axial rotations.[26,103,104] Behavioral deficits may be present at 7 days following coronal in 4-week-old piglets.[102–104] A previously published study reported the timeline of recovery of 4-week-old piglets after sagittal rapid head rotation where histopathology was obtained at 3–8 h, 1 day, 3–4 days, and 5–6 days post-injury.[101] Weeks and colleagues showed that cerebral axonal injury volume was low at 3–8 h (0.57%) then peaked at 1 day (1.15%) before decreasing at 3–4 days (0.69%) and 5–6 days (0.56%) post-injury.[101] This previous study demonstrated partial recovery of the 4-week-old piglet from diffuse axonal injury within 6 days of a sagittal injury, which justifies our choice of study time points of 1, 4, and 7 days after injury and discussion of behavioral outcomes. Human TBI studies are highly variable in their inclusion criteria, injury severity and type, and recovery duration, all of which have been shown to affect the presentation of cognitive symptoms and pathological outcomes. This heterogeneity across human EEG studies critically limits interpretation and comparison of results. Animal TBI research circumvents several of the aforementioned concerns by allowing control over injury severity and type and recovery duration. The mass-scaled equivalent angular velocity from 130 rad/sec in the 4-week-old piglet was 58 rad/sec and 38 rad/sec for the human infant and adult respectively. Rowson and colleagues[105] report a 50% risk of concussion as 28.3 rad/s using impact data from American football games.

Our mass-scaled velocity exceeded Rowson's concussion threshold. Sullivan and colleagues reported the range of sagittal head rotational angular velocity as 44–49 rad/sec from parietal and occipital head impacts during low height falls in infants,[103] which were smaller than the current study's mass-scaled equivalent, 58 rad/sec. The currently reported angular velocities prescribed to the 4-week-old piglets led to EEG changes and axonal injury that may be associated with a moderate to high risk of concussion in adult humans based on previously reported concussion thresholds. For young adults, a range of 892–1169 rad/sec^2 was reported for head angular acceleration during soccer heading impacts in both sexes.[97] Average angular acceleration (36,932 rad/sec^2) from 4-week-old piglets mass-scaled to an adult human brain mass yielded a value of 3188 rad/sec^2, which was much higher than the reported accelerations for heading a soccer ball. Significant changes to the EEG network were expected following TBI via rapid head rotation at prescribed levels.

Core network topology is influenced by frequency but not TBI

It is reported that each frequency band has a distinct network topological signature,[66] with engagement of a select combination

of electrodes placed over the left, right, frontal, parietal, temporal, or occipital brain regions. Stability of EEG functional networks was found in healthy humans for different frequency bands and across awake and sleeping states within a subject.[36] Although the spatial resolution of EEG is poor, we assume that each oscillation's characteristic network arrangement is reflective of the regional specificity of the neuronal sources. The core network topology analysis examines the influence of topology on the diffuse hyperconnectivity observed after TBI. Hyperconnectivity may occur as the result of an increase in the number of total edges, increase in edge weights, or both. We found that the presence and arrangement of the top 5% strongest edges was consistent among animals for each frequency band of interest in both groups. The core topology was dependent on the frequency, but did not change with injury or study day. This implies that the hyperconnectivity observed post-injury was not caused by the addition of core edges, but by increases in synchrony or the strengthening of core edges. The lack of addition of core edges after injury could be related to the limited axonal regenerative ability of the brain. In order to minimize total energy spent in response to TBI, previously existing cognitive and structural architecture may be utilized, as opposed to creating new connections. Hyperexcitability was found in the CA1 in 2–3-month-old Yorkshire pigs 7 days after a single coronal rapid head rotation.[99] The authors proposed that decreased axonal function leads to reduced input from afferent regions, which yields hyperexcitability in the post-synaptic neurons.

Limitations

We calculated fully connected networks because the analysis of both strong and weak connections may be critical to distinguishing between injured and uninjured networks. More complex ways of calculating synchronization networks could have been applied, such as phase lag index or mutual information, instead of cross-correlation. We chose correlation because of its ease of calculation for application to our pilot study and common usage throughout the TBI network literature. Comparing information from TBI studies in humans and piglets is difficult because of the inconsistency of data acquisition and analytical methods utilized, such as the variability in the definition of resting state used across studies. In this report, we acquired EEG from awake, immobile piglets in a quiet room free of any overt stimuli or tasks. Comparison with other resting state studies depends on the definition of ''resting state,'' which in humans is believed to constitute a mental passive state. In animal models, like human studies, we cannot be certain that we capture such a passive state, only a mental state free of overt stimuli. In human studies, subjects may be instructed to focus on a cursor,[38,88] otherwise to keep their eyes closed [48] whereas in animal studies anesthesia is often administered.[82,83] It is relevant to note that we did not train our piglets to close their eyes; therefore, comparisons with human resting state studies may be imperfect. Attention and presentation of stimuli can significantly affect the features of the EEG, but it is less clear how much these factors modulate EEG network connectivity. A second limitation of this study is that measured changes from TBI were caused only by a single, rapid non-impact injury; future studies should include and compare both focal and diffuse forms of TBI, and repeated injuries. Another limitation of this study is that pre-injury status would not be available in pediatric patients as it is in our study using piglets. However, the comparison of a single pediatric EEG to a distribution of uninjured EEGs may address cases in which pre-injury status in pediatric patients is unavailable. In our study, the comparison of pre- and post-injury status within the same animal limits the influence of inter-animal variability. We propose that future studies repeat this study with a larger sample size that identifies groupwise differences between shams/naives and injured piglets and determines whether the presence of TBI is possible with a single EEG alone. Future development of this biomarker may include its use for prognosis.

Conclusion

Changes in resting state functional network connectivity may be applicable to the precise identification of diffuse TBI (compared with controls) in children when task-related networks are difficult to obtain. Decrease in spectral power and modularity, increases in nodal strength, clustering coefficient, and global efficiency may suggest that mTBI leads to neural network damage in both cortical and white matter tract regions. Altered functional connections may be a consequence of axonal disconnection and may also be related to brain function deficits. This study serves as proof of concept that EEG networks in piglets may be helpful for the development of biomarkers that indicate when mTBI has occurred. Future studies will better clarify the relationship among resting state EEG, behavioral outcomes, and axonal injury volume in the same animals.

Acknowledgments

We thank Dr. Shanti R. Tummala for her helpful discussions on the analysis and interpretation of the data, and her valuable comments on the manuscript. We also thank Jennifer Gillard Shotto, Rewati Kulkarni, Ross Plyer, and Madeline Stolow. Funding for this study was provided by National Institutes of Health (NIH) U01 NS06945, NIH R01 NS097549, and the Stephenson Fellow and Fontaine Fellow funds.

Author Disclosure Statement

No competing financial interests exist.

References

1. Bryan, M.A., Rowhani-Rahbar, A., Comstock, R.D., Rivara, F., and Collaborative, on behalf of the S. S. C. R. (2016). Sports- and recreation-related concussions in US youth. Pediatrics 138, e20154635.
2. Faul, M., Xu, L., Wald, M., Coronado, V. (2010). *Traumatic Brain Injury in the United States: Emergency Department Visits, Hospitalizations and Deaths 2002–2006.* Centers for Disease Control and Prevention, National Center for Injury Prevention and Control: Atlanta.
3. Davis, G.A., Anderson, V., Babl, F.E., Gioia, G.A., Giza, C.C., Meehan, W., Moser, R.S., Purcell, L., Schatz, P., Schneider, K.J., Takagi, M., Yeates, K.O., and Zemek, R. (2017). What is the difference in concussion management in children as compared with adults? A systematic review. Br. J. Sports Med. 51, 949–957.
4. Nadlonek, N.A., Acker, S.N., Bensard, D.D., Bansal, S., and Partrick, D.A. (2015). Early diffuse slowing on electroencephalogram in pediatric traumatic brain injury: impact on management and prognosis. J. Pediatr. Surg. 50, 1338–1340.
5. Nuwer, M.R. (2016).Measuring outcomes for neurophysiological intraoperative monitoring. Clin. Neurophysiol. 127, 3–4
6. Schmitt, S., and Dichter, M.A. (2015). Electrophysiologic recordings in traumatic brain injury. Handb. Clin. Neurol. 127, 319–339.
7. Bartolomei, F., Bosma, I., Klein, M., Baayen, J.C., Reijneveld, J.C., Postma, T.J., Heimans, J.J., van Dijk, B.W., de Munck, J.C., de Jongh, A., Cover, K.S., Stam, C.J. (2006). Disturbed functional

connectivity in brain tumour patients: Evaluation by graph analysis of synchronization matrices. Clin. Neurophysiol. 117, 2039–2049.
8. De, V.F., Baluch, F., Astolfi, L., Subramanian, D., Zouridakis, G., Babiloni, F. (2010). Structural organization of functional networks from eeg signals during motor learning tasks. Int J Bifurc Chaos. 20, 905–912.
9. Nishida, K., Morishima, Y., Yoshimura, M., Isotani, T., Irisawa, S., Jann, K., Dierks, T., Strik, W., Kinoshita, T., Koenig, T. (2013). EEG microstates associated with salience and frontoparietal networks in frontotemporal dementia, schizophrenia and Alzheimer's disease. Clin Neurophysiol. 124, 1106–1114.
10. Boersma, M., Smit, D.J., de Bie, H.M., Van Baal, G.C., Boomsma, D.I., de Geus, E.J., Delemarre-van de Waal, H.A., and Stam, C.J. (2011). Network analysis of resting state EEG in the developing young brain: structure comes with maturation. Hum. Brain Mapp. 32, 413–425.
11. Knyazev, G.G., Savostyanov, A.N., Bocharov, A.V., Slobodskaya, H.R., Bairova, N.B. (2017). Personality and resting state networks in children: A longitudinal EEG study. Personal Individ Differ. 118, 39–43.
12. Mantini, D., Perrucci, M.G., Del, G., Romani, G.L., and Corbetta, M. (2007). Electrophysiological signatures of resting state networks in the human brain. Proc. Natl. Acad. Sci. U. S. A. 104, 13170–13175.
13. Musso, F., Brinkmeyer, J., Mobascher, A., Warbrick, T., and Winterer, G. (2010). Spontaneous brain activity and EEG microstates. a novel EEG/fMRI analysis approach to explore resting-state networks. NeuroImage 52, 1149–1161.
14. Zheng, L., Zhang, Z.-Q., Wang, Z.-G., Wang, M.-X., Yuan, C.-P., Shen, L.-F., Chen, G.-H., Yang, F., Tan, Q.-F., Jiao, Q., Lu, G.-M. (2012). EEG-fMRI study of resting-state networks in childhood absence epilepsy. Chin J Contemp Neurol Neurosurg. 12, 558–562.
15. Lind, N.M., Moustgaard, A., Jelsing, J., Vajta, G., Cumming, P., and Hansen, A.K. (2007). The use of pigs in neuroscience: modeling brain disorders. Neurosci. Biobehav. Rev. 31, 728–751.
16. Pareja, J.C.M., Keeley, K., Duhaime, A.-C., and Dodge, C.P. (2016). Modeling pediatric brain trauma: piglet model of controlled cortical impact, in: *Injury Models of the Central Nervous System*. Humana Press: New York, pps. 345–356.
17. Saito, T., Watanabe, Y., Nemoto, T., Kasuya, E., and Sakumoto, R. (2005). Radiotelemetry recording of electroencephalogram in piglets during rest. Physiol. Behav. 84, 725–731.
18. Gavilanes, A.W., Vles, J.S., von Siebenthal, K., Reulen, J.P., Nieman, F.H., van Sprundel, R., Blanco, C.E. (2001). Electrocortical brain activity, cerebral haemodynamics and oxygenation during progressive hypotension in newborn piglets. Clin Neurophysiol Off J Int Fed Clin Neurophysiol. 112, 52–59.
19. Ioroi, T., Peeters-Scholte, C., Post, I., Leusink, C., Groenendaal, F., van Bel, F. (2002). Changes in cerebral haemodynamics, regional oxygen saturation and amplitude-integrated continuous EEG during hypoxia-ischaemia and reperfusion in newborn piglets. Exp Brain Res. 144, 172–177.
20. Esslinger, C., Walter, H., Kirsch, P., Erk, S., Schnell, K., Arnold, C., Haddad, L., Mier, D., Opitz von Boberfeld, C., Raab, K., Witt, S.H., Rietschel, M., Cichon, S., and Meyer-Lindenberg, A. (2009). Neural mechanisms of a genome-wide supported psychosis variant. Science 324, 605–605
21. Armstead, W.M. (2000). Age-dependent cerebral hemodynamic effects of traumatic brain injury in newborn and juvenile pigs. Microcirculation 7, 225–235.
22. Armstead, W.M. (2005). Age and cerebral circulation. Pathophysiology 12, 5–15.
23. Buckley, N.M. (1986). Maturation of circulatory system in three mammalian models of human development. Comp. Biochem. Physiol. A Physiol. 83, 1–7.
24. Dickerson, J.W.T., and Dobbing, J. (1967). Prenatal and postnatal growth and development of the central nervous system of the pig. Proc. R. Soc. Lond. B Biol. Sci. 166, 384–395.
25. Duhaime, A.C. (1998). Age-specific therapy for traumatic injury of the immature brain: experimental approaches. Pathophysiology 5, 236.
26. Eucker, S.A., Smith, C., Ralston, J., Friess, S.H., and Margulies, S.S. (2011). Physiological and histopathological responses following closed rotational head injury depend on direction of head motion. Exp. Neurol. 227, 79–88.
27. Ibrahim, N.G., Ralston, J., Smith, C., Margulies, S.S. (2010). Physiological and pathological responses to head rotations in toddler piglets. J. Neurotrauma 27, 1021–1035.
28. Maltese, M.R. (2012). Traumatic brain injury thresholds in the preadolescent juvenile. 1–184. doi:http://repository.upenn.edu/dissertations/AAI3542829/.
29. Nuwer, M.R., Comi, G., Emerson, R., Fuglsang-Frederiksen, A., Guérit, J.M., Hinrichs, H., Ikeda, A., Luccas, F.J., and Rappelsburger, P. (1998). IFCN standards for digital recording of clinical EEG. International Federation of Clinical Neurophysiology. Electroencephalogr. Clin. Neurophysiol. 106, 259–261.
30. Modarres, M.H., Kuzma, N.N., Kretzmer, T., Pack, A.I., and Lim, M.M. (2017). EEG slow waves in traumatic brain injury: Convergent findings in mouse and man. Neurobiol. Sleep Circadian Rhythms 2, 59–70.
31. Nuwer, M. (1997). Assessment of digital EEG, quantitative EEG, and EEG brain mapping: report of the American Academy of Neurology and the American Clinical Neurophysiology Society. Neurology 49, 277–292.
32. Nuwer, M.R. (1996). Quantitative EEG analysis in clinical settings. Brain Topogr. 8, 201–208.
33. Nuwer, M.R., Hovda, D.A., Schrader, L.M., and Vespa, P.M. (2005). Routine and quantitative EEG in mild traumatic brain injury. Clin. Neurophysiol. 116, 2001–2025.
34. Fulop, S.A., and Fitz, K. (2006). Algorithms for computing the time-corrected instantaneous frequency (reassigned) spectrogram, with applications.119, 360–371.
35. MATLAB R (2015). The MathWorks Inc., Natick, MA.
36. Chu, C.J., Kramer, M.A., Pathmanathan, J., Bianchi, M.T., Westover, M.B., Wizon, L., Cash, S.S. (2012). Emergence of Stable Functional Networks in Long-Term Human Electroencephalography. J Neurosci. 32, 2703–2713.
37. Saby, J.N., and Marshall, P.J. (2012). The utility of EEG band power analysis in the study of infancy and early childhood. Dev. Neuropsychol. 37, 253–273.
38. Kramer, M. A. Eden, U.T., Lepage, K.Q., Kolaczyk, E.D., Bianchi, M.T., and Cash, S.S. (2011). Emergence of persistent networks in long-term intracranial EEG recordings. J. Neurosci. 31, 15757–15767.
39. Gazzellini, S., Napolitano, A., Bauleo, G., Bisozzi, E., Lispi, M.L., Ardu, E., Castelli, E., Benso, F. (2016). Time-frequency analyses of reaction times and theta/beta EEG ratio in pediatric patients with traumatic brain injury: A preliminary study. Dev Neurorehabilitation. 1–15.
40. Rubinov, M., and Sporns, O. (2010). Complex network measures of brain connectivity: uses and interpretations. NeuroImage 52, 1059–1069.
41. Davison, A.C., Hinkley, D.V. (1997). *Bootstrap Methods and Their Application*. 1st edition. Cambridge, NY: Cambridge University Press; 1997.
42. Gao, X. (2008). Nonparametric multiple comparison procedures for unbalanced one-way factorial designs. JSPI. 138, 2574–2591.
43. R Core Team. (2017). *R: A Language and Environment for Statistical Computing*. R Foundation for Statistical Computing: Vienna..
44. Konietschke, F., Placzek, M., Schaarschmidt, Hothorn. (2015). nparcomp: An R Software Package for Nonparametric Multiple Comparisons and Simultaneous Confidence Intervals. J Stat Softw. 64, 1–17.
45. Hillary, F.G., Slocomb, J., Hills, E.C., Fitzpatrick, N.M., Medaglia, J.D., Wang, J., Good, D.C., Wylie, G.R. (2011). Changes in resting connectivity during recovery from severe traumatic brain injury. Int J Psychophysiol. 82, 115–123.
46. Kasahara, M., Menon, D.K., Salmond, C.H., Outtrim, J.G., Tavares, J.V.T., Carpenter, T.A., Pickard, J.D., Sahakian, B.J., Stamatakis, E.A. (2011). Traumatic brain injury alters the functional brain network mediating working memory. Brain Inj. 25, 1170–1187.
47. Mayer, A.R., Mannell, M.V., Ling, J., Gasparovic, C. and Yeo, R.A. (2011). Functional connectivity in mild traumatic brain injury. Hum. Brain Mapp. 32, 1825–1835.
48. Palacios, E.M., Yuh, E.L., Chang, Y.-S., Yue, J.K., Schnyer, D.M., Okonkwo, D.O., Valadka, A.B., Gordon, W.A., Maas, A.I.R., Vassar, M., Manley, G.T., Mukherjee, P. (2017). Resting-State Functional Connectivity Alterations Associated with Six-Month Outcomes in Mild Traumatic Brain Injury. J Neurotrauma. 34, 1546–1557.

49. Rigon, A., Duff, M.C., McAuley, E., Kramer, A.F., and Voss, M.W. (2015). Is traumatic brain injury associated with reduced interhemispheric functional connectivity? A study of large-scale resting state networks following traumatic brain injury. J. Neurotrauma 33, 977–989.
50. Sharp, D.J., Beckmann, C.F., Greenwood, R., Kinnunen, K.M., Bonnelle, V., De Boissezon, X., Powell, J.H., Counsell, S.J., Patel, M.C., Leech, R. (2011). Default mode network functional and structural connectivity after traumatic brain injury. Brain J Neurol. 134, 2233–2247.
51. Risen, S.R., Barber, A.D., Mostofsky, S.H., and Suskauer, S.J. (2015). Altered functional connectivity in children with mild to moderate TBI relates to motor control. J. Pediatr. Rehabil. Med. 8, 309–319.
52. Virji-Babul, N., Hilderman, C.G.E., Makan, N., Liu, A., Smith-Forrester, J., Franks, C., Wang, Zj. (2014). Changes in Functional Brain Networks following Sports-Related Concussion in Adolescents. J Neurotrauma. 31, 1914–1919.
53. Porter, S., Torres, I.J., Panenka, W., Rajwani, Z., Fawcett, D., Hyder, A., Virji-Babul, N. (2017). Changes in brain-behavior relationships following a 3-month pilot cognitive intervention program for adults with traumatic brain injury. Heliyon. 3, e00373.
54. Slobounov, S., Gay, M., Johnson, B., and Zhang, K. (2012). Concussion in athletics: ongoing clinical and brain imaging research controversies. Brain Imaging Behav. 6, 224–243.
55. Thatcher, R.W., Biver, C., McAlaster, R., Camacho, M., and Salazar, A. (1998). Biophysical linkage between MRI and EEG amplitude in closed head injury. NeuroImage 7, 352–367.
56. Haneef, Z., Levin, H.S., Frost, J.D., and Mizrahi, E.M. (2012). Electroencephalography and quantitative electroencephalography in mild traumatic brain injury. J. Neurotrauma 30, 653–656.
57. Koufen, H., and Dichgans, J. (1978). Frequency and course of posttraumatic EEG-abnormalities and their correlations with clinical symptoms: a systematic follow up study in 344 adults [in German]. Fortschr. Neurol. Psychiatr. Grenzgeb. 46, 165–177.
58. Tebano, M.T., Cameroni, M., Gallozzi, G., Loizzo, A., Palazzino, G., Pezzini, G., and Ricci, G.F. (1988). EEG spectral analysis after minor head injury in man. Clin. Neurophysiol. 70, 185–189.
59. von Bierbrauer, A., Weissenborn, K., Hinrichs, H., Scholz, M., and Künkel, H. (1992). Automatic (computer-assisted) EEG analysis in comparison with visual EEG analysis in patients following minor cranio-cerebral trauma (a follow-up study) [in German]. EEG EMG Z. Elektroenzephalogr. Elektromyogr. Verwandte Geb. 23, 151–157.
60. Fenton, G.W. (1994).The postconcussional syndrome: new insights. J. R. Soc. Med. 87, 499–500.
61. Fenton, G.W. (1996). The postconcussional syndrome reappraised. Clin. Electroencephalogr. 27, 174–182.
62. Gosselin, N., Lassonde, M., Petit, D., Leclerc, S., Mongrain, V., Collie, A., and Montplaisir, J. (2009). Sleep following sport-related concussions. Sleep Med. 10, 35–46.
63. McClelland, R.J., Fenton, G.W., and Rutherford, W. (1994). The postconcussional syndrome revisited. J.R. Soc. Med. 87, 508–510.
64. Moeller, J.J., Tu, B., and Bazil, C.W. (2011). Quantitative and qualitative analysis of ambulatory electroencephalography during mild traumatic brain injury. Arch. Neurol. 68, 1595–1598.
65. Thompson, J., Sebastianelli, W., and Slobounov, S. (2005). EEG and postural correlates of mild traumatic brain injury in athletes. Neurosci. Lett. 377, 158–163.
66. Buzsáki, G., Logothetis, N., Singer, W. (2013). Scaling brain size, keeping timing: evolutionary preservation of brain rhythms. Neuron 80, 751–764.
67. Harmony, T. (2013). The functional significance of delta oscillations in cognitive processing. Front Integr Neurosci. 7, 1–10.
68. Fedor, M., Berman, R.F., Muizelaar, J.P., and Lyeth, B.G. (2010). Hippocampal θ dysfunction after lateral fluid percussion injury. J. Neurotrauma 27, 1605–1615.
69. Lee, D.Y., Xun, Z., Platt, V., Budworth, H., Canaria, C.A., McMurray, C.T. (2013). Distinct Pools of Non-Glycolytic Substrates Differentiate Brain Regions and Prime Region-Specific Responses of Mitochondria. Dzeja P, ed. PLoS ONE. 8, e68831.
70. Dixon, C.E., Lyeth, B.G., Povlishock, J.T., Findling, R.L., Hamm, R.J., Marmarou, A., Young, H.F., and Hayes, R.L. (1987). A fluid percussion model of experimental brain injury in the rat. J. Neurosurg. 67, 110–119.
71. Ishige, N., Pitts, L.H., Berry, I., Carlson, S.G., Nishimura, M.C., Moseley, M.E., Weinstein, P.R. (1987). The effect of hypoxia on traumatic head injury in rats: alterations in neurologic function, brain edema, and cerebral blood flow. J Cereb Blood Flow Metab. 7, 759–767.
72. McIntosh, T.K., Noble, L., Andrews, B., and Faden, A.I. (1987). Traumatic brain injury in the rat: characterization of a midline fluid-percussion model. Cent. Nerv. Syst. Trauma 4, 119–134.
73. Paterno, R., Metheny, H., Xiong, G., Elkind, J., and Cohen, A.S. (2016). Mild traumatic brain injury decreases broadband power in area CA1. J. Neurotrauma 33, 1645–1649.
74. Borich, M.R., Brown, K.E., Lakhani, B., and Boyd, L.A. (2015). Applications of electroencephalography to characterize brain activity: perspectives in stroke. J. Neurol. Phys. Ther. 39, 43–51.
75. Frieboes, R.M., Müller, U., Murck, H., von Cramon, D.Y., Holsboer, F., Steiger, A. (1999). Nocturnal hormone secretion and the sleep EEG in patients several months after traumatic brain injury. J Neuropsychiatry Clin Neurosci. 11, 354–360.
76. Parsons, L.C., Crosby, L.J., Perlis, M., Britt, T., and Jones, P. (1997). Longitudinal sleep EEG power spectral analysis studies in adolescents with minor head injury. J. Neurotrauma 14, 549–559.
77. Nakamura, T., Hillary, F.G., and Biswal, B.B. (2009). Resting network plasticity following brain injury. PloS One 4, e8220.
78. Stevens, M.C., Lovejoy, D., Kim, J., Oakes, H., Kureshi, I., Witt, S.T. (2012). Multiple resting state network functional connectivity abnormalities in mild traumatic brain injury. Brain Imaging Behav. 6, 293–318.
79. Friston, K. (2002). Functional integration and inference in the brain. Prog Neurobiol. 68, 113–143.
80. Hillary, F.G., Rajtmajer, S.M., Roman, C.A., Medaglia, J.D., Slocomb-Dluzen, J.E., Calhoun, V.D., Good, D.C., Wylie, G.R. (2014). The rich get richer: brain injury elicits hyperconnectivity in core subnetworks. PloS One. 9, e104021.
81. Hillary, F.G., Roman, C.A., Venkatesan, U., Rajtmajer, S.M., Bajo, R., Castellanos, N.D. (2015). Hyperconnectivity is a fundamental response to neurological disruption. Neuropsychology. 29, 59–75.
82. Nunez, P.L., Srinivasan, R., Fields, R.D. (2015). EEG functional connectivity, axon delays and white matter disease. Clin Neurophysiol. 126, 110–120.
83. Harris, N.G., Verley, D.R., Gutman, B.A., Thompson, P.M., Yeh, H.J., Brown, J.A. (2016). Disconnection and hyper-connectivity underlie reorganization after TBI: A rodent functional connectomic analysis. Exp Neurol. 277, 124–138.
84. Mishra, A.M., Bai, X., Sanganahalli, B.G., Waxman, S.G., Shatillo, O., Grohn, O., Hyder, F., Pitkänen, A., Blumenfeld, H. (2014). Decreased Resting Functional Connectivity after Traumatic Brain Injury in the Rat. PLoS ONE. 9, e95280.
85. Han, K., Mac Donald, C.L., Johnson, A.M., Barnes, Y., Wierzechowski, L., Zonies, D., Oh, J., Flaherty, S., Fang, R., Raichle, M.E., Brody, D.L. (2014). Disrupted modular organization of resting-state cortical functional connectivity in U.S. military personnel following concussive ''mild'' blast-related traumatic brain injury. NeuroImage. 84, 76–96.
86. Alexander-Bloch, A.F., Gogtay, N., Meunier, D., Birn, R., Clasen, L., Lalonde, F., Lenroot, R., Giedd, J., Bullmore, E.T. (2010). Disrupted modularity and local connectivity of brain functional networks in childhood-onset schizophrenia. Front Syst Neurosci. 4, 147.
87. Pevzner, A., Izadi, A., Lee, D.J., Shahlaie, K., and Gurkoff, G.G. (2016). Making waves in the brain: what are oscillations, and why modulating them makes sense for brain injury. Front. Syst. Neurosci. 10, 30.
88. Luo, Q., Xu, D., Roskos, T., Stout, J., Kull, L., Cheng, X., Whitson, D., Boomgarden, E., Gfeller, J., Bucholz, R.D. (2013). Complexity Analysis of Resting State Magnetoencephalography Activity in Traumatic Brain Injury Patients. J Neurotrauma. 30, 1702–1709.
89. Douw, L. Schoonheim, M.M., Landi, D., van der Meer, M.L., Geurts, J.J., Reijneveld, J.C., Klein, M., and Stam, C.J. (2011). Cognition is related to resting-state small-world network topology: an magnetoencephalographic study. Neuroscience 175, 169–177.
90. Olsen, K.S., Madsen, P.L., Børme, T., and Schmidt, J.F. (1993). The effect of ketanserin on cerebral blood flow and oxygen metabolism in healthy volunteers. Acta Neurochir. (Wien) 125, 83–85.
91. Cucchiara, R.F., Theye, R.A., and Michenfelder, J.D. (1974). The effects of isoflurane on canine cerebral metabolism and blood flow. Anesthesiology 40, 571–574.
92. Todd, M.M., and Weeks, J. (1996). Comparative effects of propofol, pentobarbital, and isoflurane on cerebral blood flow and blood volume. J. Neurosurg. Anesthesiol. 8, 296–303.

93. Kochs, E., Hoffman, W.E., Werner, C., Albrecht, R.F., and Schulte am Esch, J. (1993). Cerebral blood flow velocity in relation to cerebral blood flow, cerebral metabolic rate for oxygen, and electroencephalogram analysis during isoflurane anesthesia in dogs. Anesth. Analg. 76, 1222–1226.
94. Gelman, S., Fowler, K.C., and Smith, L.R. (1984). Regional blood flow during isoflurane and halothane anesthesia. Anesth. Analg. 63, 557–565.
95. Smith, J.H., Karsli, C., Lagacé, A., Luginbuehl, I., Barlow, R., and Bissonnette, B. (2005). Cerebral blood flow velocity increases when propofol is changed to desflurane, but not when isoflurane is changed to desflurane in children. Acta Anaesthesiol. Scand. 49, 23–27.
96. O'Connor, C.A., Cernak, I., and Vink, R. (2003). Interaction between anesthesia, gender, and functional outcome task following diffuse traumatic brain injury in rats. J. Neurotrauma 20, 533–541.
97. Statler, K.D., Kochanek, P.M., Dixon, C.E., Alexander, H.L., Warner, D.S., Clark, R.S. b., Wisniewski, S.R., Graham, S.H., Jenkins, L.W., Marion, D.W., Safar, P.J. (2000). Isoflurane Improves Long-Term Neurologic Outcome Versus Fentanyl After Traumatic Brain Injury in Rats. J Neurotrauma. 17, 1179–1189.
98. Hertle, D., Beynon, C., Zweckberger, K., Vienenkötter, B., Jung, C.S., Kiening, K., Unterberg, A., Sakowitz, O.W. (2012). Influence of Isoflurane on Neuronal Death and Outcome in a Rat Model of Traumatic Brain Injury. In: *Intracranial Pressure and Brain Monitoring XIV*. Springer: Vienna. pps 383–386.
99. Bruins, B., Kilbaugh, T.J., Margulies, S.S., and Friess, S.H. (2013). The anesthetic effects on vasopressor modulation of cerebral blood flow in an immature swine model. Anesth. Analg. 116, 838–844.
100. Brady, K.M., Lee, J.K., Kibler, K.K., Easley, R.B., Koehler, R.C., Czosnyka, M., Smielewski, P., Shaffner, D.H. (2009). The lower limit of cerebral blood flow autoregulation is increased with elevated intracranial pressure. Anesth Analg. 108, 1278–1283.
101. Weeks, D., Sullivan, S., Kilbaugh, T., Smith, C., and Margulies, S.S. (2014). Influences of developmental age on the resolution of diffuse traumatic intracranial hemorrhage and axonal injury. J. Neurotrauma 31, 206–214.
102. Atlan, L.S., Smith, C., Margulies, S.S. (2017). Improved prediction of direction-dependent, acute axonal injury in piglets. J Neurosci Res. 96, 536–544.
103. Sullivan, S., Friess, S.H., Ralston, J., Smith, C., Propert, K.J., Rapp, P.E., and Margulies, S.S. (2013). Behavioral deficits and axonal injury persistence after rotational head injury are direction dependent. J. Neurotrauma 30, 538–545.
104. Sullivan, S., Friess, S.H., Ralston, J., Smith, C., Propert, K.J., Rapp, P.E., and Margulies, S.S. (2013). Improved behavior, motor, and cognition assessments in neonatal piglets. J. Neurotrauma 30, 1770–1779.
105. Rowson, S., Duma, S.M., Beckwith, J.G., Chu, J.J., Greenwald, R.M., Crisco, J.J., Brolinson, P.G., Duhaime, A.C., McAllister, T.W., and Maerlender, A.C. (2012). Rotational head kinematics in football impacts: an injury risk function for concussion. Ann. Biomed. Eng. 40, 1–13.

Address correspondence to:
Susan S. Margulies, PhD
Georgia Tech
The U.A. Whitaker Biomedical Engineering Building
313 Ferst Drive
Atlanta, GA 30332-0535

E-mail: susan.margulies@gatech.edu